INSTITUTE
FOR
AEROSPACE STUDIES

UNIVERSITY OF TORONTO

ON THE MODALITY OF FATIGUE ENDURANCE DISTRIBUTIONS IN OFHC COPPER

by

G. K. Korbacher

June, 1970.

UTIAS Report No.145

ON THE MODALITY OF FATIGUE ENDURANCE DISTRIBUTIONS IN OFHC COPPER

by

G. K. Korbacher

Manuscript received October, 1969.

June, 1970. UTIAS Report No.145

ABSTRACT

Unaccounted scatter of fatigue endurances, discontinuities (knees) in S (Stress) - N (Life) curves, metallographic evidence for the action of more than one fatigue mechanism and semi-statistical endurance data which indicates the coexistence of more than one endurance distribution at a given stress level strongly imply that S-N curves cannot, as conventionally done, be represented realistically by a monolithic single analytical relation of exponential form. In particular, Swanson's semi-statistical endurance data, his interpretation of the knees as a cross-over region from one predominant endurance distribution to another and its implications on the S-N curve shape, on fatigue life scatter and on the responsible fatigue mechanisms warranted further investigation.

Altogether 884 OFHC copper specimens were fatigued under axial-load of 10, 12.7, 13, 14, 16.5 and 19 ksi constant amplitude and zero mean stress. Log-normal, extreme value, combinations of two truncated log-normal and truncated log-normal and extreme value distribution functions were fitted to the experimental endurance distributions. Furthermore, a mathematical dissection method was applied.

The main results of this study are:

1. The two endurance distributions observed with alloys could not be verified for polycrystalline (OFHC) copper

2. At stress levels around the lower knee the existence of two modes (bimodality) was apparent

3. At stress levels well above the knee, endurance distributions seem to become single log-normal, below the knee extremal

4. The bimodality seems to be caused by a transition of predominance from one to another fatigue mechanism (Wood's F to H range transition).

In conclusion, it may be said that the most important factor responsible for either the single, bimodal or two endurance distribution phenomenon seems to be the microstructural response of the tested material to the acting stress level. However, also our tests do not permit us to draw definite conclusions.

TABLE OF CONTENTS

NOTATION

b	Weibull shape parameter
E	Young's Modulus
f(x)	frequency distribution function or probability density function (p.d.f.)
F(x)	cumulative probability function or cumulative distribution function (c.d.f.)
ksi	thousands of pounds per square inch
LTF	Long Term Fatigue - designating the high-endurance component in a bimodal distribution
$\log_{10}$, log	common logarithm
ln	natural logarithm
n	total number of specimens in the sample of a population
n_{tr}	number of observations, the endurance values of which are known in a truncated sample
N	endurance of a specimen in cycles
N_i	The ith ordered endurance when the endurance values of a sample are arranged in ascending sequence
N_o	the minimum life parameter, N_o is defined by $F(N \leq N_o)=0$
psi	pounds per square inch
P_i	plotting position
r	correlation coefficient
STF	Short Term Fatigue - designating the low-endurance component in a bimodal distribution
s^2	Estimate of σ^2 obtained from a sample, sample variance
s	sample standard deviation, estimate of σ
S_a	nominal stress amplitude in ksi
V	characteristic life parameter in Weibull distribution defined by $F(V) = 1/e$.
X	$\text{Log}_{10}(N)$
$\bar{X}$	Mean of X_i, given by $\bar{X} = 1/n \sum_{i=1}^{n} X_i$

X_i	the ith ordered value of X
α	scale parameter of Weibull distribution being equal to $(V-M_o)$
β	shape parameter of Weibull distribution (same as b)
x_o	location parameter of Log Weibull distribution
σ^2	variance of a population
σ	population standard deviation
u	population mean
λ_i	ith cumulant or semi-invariant

I. INTRODUCTION

Humps or discontinuities in fatigue S-N curves were observed during the last decade for many metals under various testing conditions. Finney (Ref. 1), in 1967, (thoroughly reviewed all publications on this phenomenon, outlined the factors which influence it, and critically discussed the theories advanced as an explanation of this phenomenon. However, his paper leaves no doubt that we are still far from being able to properly explain this phenomenon and that, in Finney's words "the phenomenon highlights the need for research into the basic mechanisms of fatigue failure ...". In particular the significance of statistical fatigue testing on the hump or discontinuity phenomenon is not yet sufficiently investigated as to the light, this kind of testing can throw on the acting fatigue mechanisms, which are responsible for causing this phenomenon. The purpose of the work reported in this paper explores this aspect.

Even though much data on the conventional stress (S) - endurance (N) relation can be found for design purposes, not enough attention has been paid to the statistical nature of fatigue and its repercussions on the S-N relation. Taking proper account of the statistical nature of fatigue actually necessitates interpreting the S-N relation in terms of probability, the probability (P) that a structure subjected to a certain stress will fail at or before a specified number of cycles (N) is reached. Since for practical and economical reasons, zero probability of failure designs are out of question, the "true" risk for any value of $P > 0$ depends, besides on P itself, also on the accuracy to which the endurance distribution at the design stress level is known.

Semi-statistical fatigue test results suggest that the familiar way of expressing either the entire S-N curve, or large portions of it by a single power function is suspect. Furthermore, they suggest that the "true" S-N relation is the product of the action and interaction of several fatigue mechanisms, one predominating below the lower knee of the S-N curve, one above it and a third acting in the region of very high stresses and alternating plasticity. Recent tests with semi-statistical specimen numbers by Swanson (Ref. 2) using aluminum and Cicci (Ref. 3) using steel support this evidence and Swanson concluded that the action of the individual fatigue mechanisms, where they compound, as for instance in the transition region around the lower knee of the S-N curve, leads to the observed large scatter in the fatigue endurances due to the blending of two endurance distributions, each being the result of one or the other of two coexisting failure mechanisms. One mechanism is believed to cause failure predominantly above, the other predominantly below the knee, the knee being the transition region in which the higher probability for failure occurrence gradually switches from one to the other fatigue failure mechanism.

Another observation made at stress levels around the lower knee of the S-N curve concerned the endurance distributions. At high stress levels, they seem to be best represented by log-

normal (Gaussian) distribution functions. At low stress levels, extreme value (Weibull) distribution functions seem to fit better. All these functions fit generally best near the mode of the endurance distributions. At the lower knee, however, neither function fits too well because of the strongly enhanced endurance scatter, the result of the blending and transition of the two observed endurance distributions.

The action of more than one and the transition from one to another fatigue failure mechanism is also well demonstrated metallographically. Wood (Refs. 4 and 5) detected microstructural differences as a function of strain amplitude, which led him to divide the conventional S-N curve into three amplitude ranges known as H, F, and S. Frost (Ref. 6) observed a transition from slip band microcracking at stress levels below the knee to grain boundary microcracking at stress levels above it.

All the above described phenomena focus attention to the lower knee region of the S-N curve about which Dolan (Ref. 7) once said that it is one of the main problem areas in fatigue, requiring special attention and further examination.

II. STATE OF THE ART

The above said demonstrates that there is, as yet, no fundamental physical model of fatigue, which adequately presents the change in endurance behaviour with stress level and accounts for the statistical discoveries, regarding the nature of overlapping and transition between various fatigue mechanisms. This lack of a model is often hampering and critical, especially in attempts to establish fatigue damage accumulation laws.

Of the various theories for fatigue damage accumulation laws proposed by, e.g., Freudenthal, Weibull, Cortan-Dolan, most are being based on a monolithic stress-endurance relation throughout the stress range. This monolithic relation, usually represented by a single analytical function, results from the visual smoothing of scant endurance data and is typically of exponential form. While the exact form of the basic but "true" S-N relation is of vital importance for the theoretical development of adequate fatigue damage laws, it is a curious fact that very few high quality (statistical) experimental investigations of this relation exist, despite the plethora of S-N data generated in the literature. However, already the few semi-statistical investigations which had been carried out (see e.g., Refs. 2, 3, 8 and 9) prior to proper statistical testing at the Institute for Aerospace Studies, University of Toronto (UTIAS), strongly suggested that for polycrystalline materials and alloys:

(a) The fatigue stress-endurance relations is the result of a statistical phenomenon and must be treated as such.

(b) The use of a single analytical expression to describe this relation throughout the macroelastic stress range is undoubtedly an oversimplification of what is actually happening.

I. INTRODUCTION

Humps or discontinuities in fatigue S-N curves were observed during the last decade for many metals under various testing conditions. Finney (Ref. 1), in 1967, (thoroughly reviewed all publications on this phenomenon, outlined the factors which influence it, and critically discussed the theories advanced as an explanation of this phenomenon. However, his paper leaves no doubt that we are still far from being able to properly explain this phenomenon and that, in Finney's words "the phenomenon highlights the need for research into the basic mechanisms of fatigue failure ...". In particular the significance of statistical fatigue testing on the hump or discontinuity phenomenon is not yet sufficiently investigated as to the light, this kind of testing can throw on the acting fatigue mechanisms, which are responsible for causing this phenomenon. The purpose of the work reported in this paper explores this aspect.

Even though much data on the conventional stress (S) - endurance (N) relation can be found for design purposes, not enough attention has been paid to the statistical nature of fatigue and its repercussions on the S-N relation. Taking proper account of the statistical nature of fatigue actually necessitates interpreting the S-N relation in terms of probability, the probability (P) that a structure subjected to a certain stress will fail at or before a specified number of cycles (N) is reached. Since for practical and economical reasons, zero probability of failure designs are out of question, the "true" risk for any value of $P > 0$ depends, besides on P itself, also on the accuracy to which the endurance distribution at the design stress level is known.

Semi-statistical fatigue test results suggest that the familiar way of expressing either the entire S-N curve, or large portions of it by a single power function is suspect. Furthermore, they suggest that the "true" S-N relation is the product of the action and interaction of several fatigue mechanisms, one predominating below the lower knee of the S-N curve, one above it and a third acting in the region of very high stresses and alternating plasticity. Recent tests with semi-statistical specimen numbers by Swanson (Ref. 2) using aluminum and Cicci (Ref. 3) using steel support this evidence and Swanson concluded that the action of the individual fatigue mechanisms, where they compound, as for instance in the transition region around the lower knee of the S-N curve, leads to the observed large scatter in the fatigue endurances due to the blending of two endurance distributions, each being the result of one or the other of two coexisting failure mechanisms. One mechanism is believed to cause failure predominantly above, the other predominantly below the knee, the knee being the transition region in which the higher probability for failure occurrence gradually switches from one to the other fatigue failure mechanism.

Another observation made at stress levels around the lower knee of the S-N curve concerned the endurance distributions. At high stress levels, they seem to be best represented by log-

normal (Gaussian) distribution functions. At low stress levels, extreme value (Weibull) distribution functions seem to fit better. All these functions fit generally best near the mode of the endurance distributions. At the lower knee, however, neither function fits too well because of the strongly enhanced endurance scatter, the result of the blending and transition of the two observed endurance distributions.

The action of more than one and the transition from one to another fatigue failure mechanism is also well demonstrated metallographically. Wood (Refs. 4 and 5) detected microstructural differences as a function of strain amplitude, which led him to divide the conventional S-N curve into three amplitude ranges known as H, F, and S. Frost (Ref. 6) observed a transition from slip band microcracking at stress levels below the knee to grain boundary microcracking at stress levels above it.

All the above described phenomena focus attention to the lower knee region of the S-N curve about which Dolan (Ref. 7) once said that it is one of the main problem areas in fatigue, requiring special attention and further examination.

II. STATE OF THE ART

The above said demonstrates that there is, as yet, no fundamental physical model of fatigue, which adequately presents the change in endurance behaviour with stress level and accounts for the statistical discoveries, regarding the nature of overlapping and transition between various fatigue mechanisms. This lack of a model is often hampering and critical, especially in attempts to establish fatigue damage accumulation laws.

Of the various theories for fatigue damage accumulation laws proposed by, e.g., Freudenthal, Weibull, Cortan-Dolan, most are being based on a monolithic stress-endurance relation throughout the stress range. This monolithic relation, usually represented by a single analytical function, results from the visual smoothing of scant endurance data and is typically of exponential form. While the exact form of the basic but "true" S-N relation is of vital importance for the theoretical development of adequate fatigue damage laws, it is a curious fact that very few high quality (statistical) experimental investigations of this relation exist, despite the plethora of S-N data generated in the literature. However, already the few semi-statistical investigations which had been carried out (see e.g., Refs. 2, 3, 8 and 9) prior to proper statistical testing at the Institute for Aerospace Studies, University of Toronto (UTIAS), strongly suggested that for polycrystalline materials and alloys:

(a) The fatigue stress-endurance relations is the result of a statistical phenomenon and must be treated as such.

(b) The use of a single analytical expression to describe this relation throughout the macroelastic stress range is undoubtedly an oversimplification of what is actually happening.

(c) The stress-endurance relation is not due to a single fatigue mechanism. When enough lives are obtained at a given stress level in the region of the lower 'knee' of the S-N curve, almost invariably these endurances can be grouped quite naturally into at least two separate distributions. This can be seen in test results going back to 1928 (see Ref. 9).

(d) In many cases an orderly rise of the first and decay of the second distribution developed as the stress amplitude was raised. As a result, the 'knee' of the S-N curve is really a 'cross-over' region representing a transition from one predominant distribution to the other. The final shape of the S-N curve in this knee region is merely the outcome of the superposition of two separate fatigue processes.

(e) These statistical observations are not without support from more fundamental fatigue studies. Freudenthal, Lazan and Wood (Refs. 10, 11 and 4, respectively) have made physical and metallurgical observations which led them to surmise that the shape of the S-N curve results from two distinctly different mechanisms in the region of the lower knee of the S-N curve.

(f) There is a third mechanism, or group of mechanisms, operative at stresses above the macroelastic (static) stress range and responsible for a distinctly different stress-endurance behaviour. D'Amato (Ref. 12) and Coffin (in many papers) have demonstrated that this stress-endurance relation is distinctly different from the lower knee one, and usually exhibits a strain-endurance straight line relation with a slope of -1/2 on a log-log plot. It is apparent from Ref. 13 that the transition region (often designated as the "upper" knee) between these stress levels and lower stresses exhibits overlapping characteristics rather similar to those found at the lower 'knee' of the S-N curve. Porter and Levy have grouped the endurance data in the same manner as has been done at WPAFB. However, metallurgical studies of the test material used in both cases have not been productive of a firm correlation with the statistical behaviour.

(g) Finally, it might be added that the same type of phenomenon has also been observed in the development of creep-rupture data with stress level (Ref. 14). The author of this reference pointed out that test results obtained at V.D.E.H., Düsseldorf, Germany, showed a very similar trend. The usually assumed 'point of inflexion' of the creep-rupture curve (stress versus log time) is actually a region wherein two rupture lines cross over. This is contrasted with the usual assumption that the creep process is singular and follows a parametric relation (such as the Larson-Miller relation) to yield a single rupture line or curve. Earlier tests described in Ref. 15, show that a Z-shaped

creep rupture curve (with a discontinuity) is formed when only a few test results are obtained. This is completely analogous to the behaviour of fatigue results as discussed in Ref. 9.

(h) In spite of the evidential support which statistical observations received from metallurgical evidence, attempts to correlate both have not been productive yet.

III. ON THE DUALITY OF FATIGUE FAILURE MECHANISMS

Freudenthal and Gumbel (Ref. 16) have asserted that an acceptable fatigue theory should account for localized 'high' temperatures developed in the course of the reversed slip process. They point out that many fundamental observations regarding fatigue at the microscopic level such as softening, reversion, depletion, discolouration, point to temperature peaks in the metal at the nuclei of microcracks. Other factors such as hysteresis, fretting, and the observed analogous behaviour of creep-rupture data point also to thermally-activated processes.

While Broom (page 755, Ref. 17) has raised objections to the actual magnitude of these temperatures, it does appear that thermal effects could exist (page 904, Ref. 17). Certainly there are many examples of improved fatigue resistance at low temperatures (Ref. 18), and perhaps the important factor may be the existence of sizeable temperature gradients (Coates, page 880, Ref. 17) rather than the actual magnitude of the temperature, or the combination of both, that is important.

When one looks for further analogues with regard to a thermally activated fatigue process, the kinetic behaviour of incoherent particles, such as molecules in a gas comes to mind. It is known that this behaviour in a gas leads to a Maxwell-Boltzmann distribution of velocity components. The density function of this distribution has the form

$$f(x) = A\, x^2\, e^{-x^2}$$

In the development of his 'heat flash' theory, Freudenthal took a different approach and postulated the 'weak link' principle for fatigue. This leads to the Weibull distribution, which has the general form (for its density function) of

$$f(x) = A\, x^{b-1}\, e^{-x^b}$$

It can be seen that these two distributions are fundamentally quite different. Yet the determination of goodness of fit, to establish one distribution over the other, should be possible from proper statistical test data such as reported on below.

It is felt that while the weak link principle may apply to crack' propagation, the incoherent nature of crack nucleus development in crack initiation may be better represented by the

Maxwell-Boltzmann relation. That such a distribution should reveal itself in actual failures (which must involve some period of crack propagation) is possible, since with axial constant load testing, such a propagation can be catastrophic and can occur, as actually observed in our own test series, in very few cycles. For this reason it may be possible to establish a fatigue model of some considerable soundness, for the crack initiation process at least, from high-quality statistical studies alone.

The duality of the fatigue mechanism as exhibited by Constant Amplitude test results below the 'plasticity' range can be appreciated from the metallurgical observations of two fatigue processes as discussed by Freudenthal (Ref. 10), Wood (Ref. 4) and Lazan (Ref. 11). Using the terms STF and LTF again, the following observations are pertinent:

1. The term STF appears to apply to observations of "high level fatigue" (Freudenthal), "H type" Mechanism (Wood) and "fatigue above the sensitivity limit" (Lazan), while the LTF mechanism applies to "low stress fatigue", "F-type" and fatigue below the "sensitivity limit" respectively. The position of Lazan's sensitivity limit for 2024-T4 material is 89% of the endurance limit stress. This probably represents the highest level at which the LTF mechanism predominates. Above this level, the effect of the STF mechanism is probably able to mask the effect of the small populations of LTF since no attempt to distinguish between these distributions was made in the assessment of the endurance limit stress level.

2. The STF Mechanism

   (a) is "akin to that observable in unidirectional static deformation", and may be related to a critical amount of strain hardening (Freudenthal).

   (b) causes failure by increasing internal stresses in a coarse-slip manner similar to that obtained from static deformation, and strain hardening is progressive to failure (Wood).

   (c) possesses damping which is apparently a function of the prior stress history as well as the stress level (i.e. varies with the number of applied cycles) (Lazan).

   (d) results in the release of latent energy (in the microstructure) predominantly at the recovery temperature as well as the recrystallization temperature (Freudenthal).

   (e) causes cracks which are usually of irregular shape and include grain boundaries, due to their interaction with micro-residual stress field at the work-hardened structure (Freudenthal).

(f) primarily causes grain boundary microcracking (Frost).

3. The LTF Mechanism

(a) produces considerably less strain hardening and no significant distortion, but a multitude of fine slip bands congregated in striations. As a result of reduced strain hardening, the total sum of permanent deformations to failure can attain any value, being clearly unrelated to the fatigue phenomenon (Freudenthal).

(b) causes failure by producing abnormal distortion along operative or localized fine slip zones, and subsequently creating surface irregularities (peaks and notches) which lead to eventual failure in the weakened areas. Strain hardening is insignificant (Wood).

(c) possesses a damping versus Constant Amplitude stress relation that is log-log linear, and the mechanism "displays no history effect". (Lazan).

(d) causes transition from grain boundary microcracking at STF to slip band microcracking at LTF.

(e) results in the release of latent energy in a diffuse manner over the whole temperature range (Freudenthal).

(f) causes cracks which are concentrated within the striations (Freudenthal).

(g) may impose a distinctive mode of deformation characteristic of its loading, i.e., stressing at small micro-plastic amplitudes (Wood).

Further evidence of both a metallurgical nature and and statistical nature may be found in Reference 9.

IV. AIMS OF CONDUCTED RESEARCH

It was against the background of Sections II and III, that in 1964 at UTIAS, a program was started with the following aims in mind: (1) a careful determination of the S-N relation, in the stress range which contains the lower knee, on a proper statistical basis.

(2) to disprove or confirm on a proper statistical basis that the lives of fatigued specimens fall into two distinctly different endurance distributions (co-existing or bimodal).

(3) to investigate and identify, if possible, the characteristics of the fatigue mechanisms involved and responsible for the observed separation or bimodality of the endurance distributions.

(4) to try to correlate the statistically observed failure

mechanisms with Wood's H and F range fatigue mechanisms. If such a correlation could be established it could show that the lower knee corresponds to the intersection of the H with the F range line.

(5) to identify some of the parameters which influence, induce or force specimens to fail either under the short term (STF) or long term (LTF) fatigue mechanism.

V. MATERIAL, FATIGUE MACHINES AND TEST PROCEDURE

5.1 Material

Specimens used for these tests were of certified OFHC copper-ASTM Specification B-170-47 of better than 99.96% purity. These specimens (see Fig.1) were rough machined, annealed, hanging (2 hrs. at 1050°F in vacuum) in batches of 200 each and fine machined (5 lathe cuts of 0.0025 in. depth and 0.002 in. feed per revolution). Specimens showing eccentricity of more than 0.001 in. were excluded from testing. In spite of the utmost possible care to avoid surface work-hardening during the final machining, a layer to close to 0.01 in. was detected which could not be removed entirely by subsequent mechanical and electro-polishing. For further details on material specification and properties, annealing and specimen preparation, see Refs. 19 and 20. The average grain size of all heat treatment batches was that of ASTM No.8 (about 0.027 mm grain diameter).

5.2 Fatigue Machines

The fatigue testing machines used for this study were of the resonance type, tension-compression (Fig.2). The bulk of the testing (784 specimens) was done with machine No.1 (25 lb electromagnetic shaker, see Ref.19), the remaining 100 specimens - because of the high load requirement - with machine No.2 (50 lb shaker, see Ref.21 for details). The operating (resonance) frequency was 60-80 cps or 48 cps for machine No.1 and 2, respectively. The gripping heads used "rubber-flex" collets in conical bores, holding the specimens very firmly and without slippage.

The load monitoring system consisted of strain-gauged dynamometer springs, a pre-amplifier and an electronic voltmeter for load amplitude indication. The dynamometer signal actuated a photoelectric device with two cutout points, one to warn (buzzer) against low load, the other one to shut off the machine just before the specimen fails. The load was applied via an audio oscillator, the sine wave output of which was amplified and fed to the electromagnetic shaker. For further details about cycle counting, fatigue machine alignment and calibration, test accuracy and repeatability, see Ref.19. The maximum error in the applied dynamic load was estimated to be about 1.5%. This accurac y is qualitatively confirmed by the endurance data obtained for the 12.7 and 13 ksi stress levels. The merely 2.4% increase in stress amplitude showed (see Fig. 8 of Ref.19) an absolutely unequivocal separation of the endurance data.

5.3 Test Procedure

The greatest care was taken to ensure that tested specimens were as identical as they could be produced under very stringent requirements. Equal care was employed to keep experimental errors to an ab solute minimum.

All specimens fatigued at one particular stress level were taken from one and the same heat treatment batch. After gripping the specimens and starting the tests, the applied load had to be reduced continuously during the first 3 minutes to compensate for the extensive strain-hardening in the specimens. Simultaneously, the resonance frequency needed slight adjustment. Later on in high or low load tests, load re-adjustments were needed at 15 to 20 minutes or 2-3 hour intervals, respectively. The amount of heat produced in the specimens due to energy dissipation at the higher load levels was very noticeable. For further details, see Refs. 19 and 21.

Table I below indicates the number of specimens fatigued at each stress level, the machine used, and from which heat treatment batch the specimens were taken.

STRESS LEVEL ksi	NO. OF SPECIMENS	MACHINE NO.	FROM HEAT TREATMENT BATCH	FOR DETAILS (SEE REF.)
± 10	3	1	F	21
± 12.7	148	1	D	19
± 13	148	1	B	19
± 14	133	1	A	19
± 16.5	200	1	C	19
± 16.5	150	1	F	21
± 19	84	2	E	21
± 19	16	2	G	21

All tests were done at room temperature and uncontrolled room humidity. Both were continuously recorded. While no correlation was apparent between temperature and endurances, Fig. 3. shows that there is a slight correlation between humidity and endurances. Lower fatigue lives seem to be more frequent at higher values of relative humidity.

5.4 Properties of Unfatigued Specimens

From each annealing batch, 5 specimens were hardness tested, X-rayed, and subjected to a tension test. The results are given in Tables I of Refs. 19 and 21, including the arithmetic

means. For the more important properties, the standard deviations and the 95% confidence limits are also listed. A microstructural analysis of the control specimens showed a partially recrystallized structure, being about 50% polygonized.

VI. METHODS OF STATISTICAL ANALYSIS

The evidence of two well separated endurance distributions (see e.g., Refs. 2 and 3) for alloyed metals at stress levels around the lower knee of the S-N curve and the assumption of more than one operating failure mechanism (see e.g. Refs. 4, 10 and 11) leads to the concept of a heterogeneous endurance population, i.e., an endurance distribution having more than one mode.

6.1 Histograms

All test endurances were plotted in histogram form, using a class length of 0.01 log N. For the 13 and 14 ksi stress levels the histograms to the left of the distribution peak indicated a valley, which was less well defined at both the lower and higher stress levels. This is demonstrated in Figs. 4, 5 and 6. In general, histograms for overlapping distributions - dependent on the number of specimens plotted - were found rather ambiguous to draw conclusions as to the type of distribution (single or bimodal).

6.2 Statistical Data-Tabulation

All fatigue endurances observed at the stress levels listed in Table I of Sec. 5.3 are tabulated in either Refs. 19 or 21.

6.3 Distribution Functions Applied to Test Data

Table II below shows the distribution functions or methods of analysis which were applied to the test data of Haagensen and Ravindran.

TABLE II

STRESS LEVEL	NO. OF SPECIMENS	ANALYSIS (see key below)	FOR DETAILS (see Ref.)
± 10	3	None	21
± 12.7	148	A, B-1, B-2, C-1	19
± 13	148	A, B-1, B-2, C-1, C-2	19
± 14	133	A, B-1, B-2, C-1, C-2	19
± 16.5	200	A, B-1, B-2, C-1	19
± 16.5	150	A, B-2, C-1, D	21
± 19	100	A, B-2, C-1, D	21
± 16.8	973	A, B-2, C-1	21
Rotating Bending	(notched AL)		Test Data: Bloomer & Roylance (Ref. 22)

KEY TO ANALYSES OF TABLE II

DESIGNATION		DISTRIBUTION FUNCTION OR METHOD OF ANALYSIS
A	=	Single log-normal distribution
B	=	Single Weibull (extreme value) distribution
B-1	=	Classical moment method
B-2	=	Method of upper vertical moments
C	=	Truncated log-normal distribution
C-1	=	High-endurance part excluded
C-2	=	Low-endurance part excluded
D	=	Mathematical dissection method (see Appendix B of Ref.21)

VII. RESULTS OF STATISTICAL ANALYSES

7.1 Single Log-Normal Distributions

The pertinent parameters, x, s and r (see NOTATIONS) were calculated. They are listed in Table III below:

TABLE III

PARAMETERS OF SINGLE LOG-NORMAL DISTRIBUTION

	12.7 ksi 148 specim.	13.0 ksi 148 speci.	14.0 ksi 133 speci.	16.5 ksi 200 specim.
Mean of log (N), $\bar{X}$	6.17725	6.10949	5.66479	5.32034
Standard deviation, s	0.099334	0.095913	0.099089	0.1020987
Correlation coeff., r	0.99044	0.99330	0.98726	0.99668

	16.5 ksi 150 specim.	16.5 ksi 350 specim.	19.0 ksi 100 specim.
Mean of log (N), $\bar{X}$	5.32089	5.32058	4.85163
Standard deviation, s	0.0704147	0.0903587	0.0510833
Correlation coeff., r	0.99712	0.99918	0.97805

Typical endurance data for some of the above stress levels are plotted as single distributions on log-normal probability paper in Figs. 7 and 8. The solid lines in the plots are the linear regression lines (from method of least squares).

The standard deviations (see Tab le III) and the slopes of the regression lines show that the variance of the endurances at the 12.7 ksi stress level is in general higher than that at the higher stress levels. This decrease in scatter, with increasing stress is what one conventionally expects (for alloys). For the 16.5 ksi and 19 ksi stress level (see Figs. 7 and 8), the endurances very closely fit the single distribution regression line, suggesting that the sample is drawn from a single normal population. For the lower stress levels (14 and 13 ksi), endurances do not fit the regression line as well. Actually, the endurances could be better represented by two straight lines, one for failure

probabilities below, the other one above the 30 to 40% point (see dashed lines in Fig.7). The dashed lines were fitted visually. Their difference in slope suggests that the endurance distribution may have two components, the component of low failure probability having a smaller variance than the one of high probability. The heterogeneous nature of specifically the 13 and 14 ksi endurance distributions is also illustrated in their histograms (see e.g., Fig.6).

For the 12.7 ksi stress level (Fig.7), the endurances fit neither the regression line near the two straight line concept well, However, the endurances seem to follow a smooth curve fairly well. This could be taken to mean that a three-parameter distribution function could provide a better fit, as Fig.9 actually confirms. Obviously the Weibull (upper vertical moment) distribution function provides the best fit. Note that the distribution functions of Fig. 9 were calculated for the distribution of N (not log N, the abscissa of Fig.9) cycles. The correlation coefficients given elsewhere for these distribution functions do therefore not apply to Fig.9.

7.2 Single Weibull (Extreme Value) Distributions

7.2.1 Classical Moment Method

Using the procedure outlined in Appendix 3 of Ref. 19, the skewness parameter was calculated with the aid of an IBM 7090/7094-11 computer. For further details see Ref. 19. All the calculated Weibull parameters and correlation coefficients are shown below in Table IV.

TABLE IV

PARAMETERS OF SINGLE WEIBULL DISTRIBUTION

(Classical Moment Method)

	148 (12.7) specim.	148 (13) specim.	133 (14) specim.	200 (16.5) specim.
Shape parameter, b	2.53	1.76	1.525	2.28
Minimum life, N_o (mill. cycles)	0.62529	0.8046	0.303241	0.105766
Characteristic life, V (mill. cycles)	1.64879	1.38228	0.493641	0.229114
Correlation coefficient, r	0.99554	0.99195	0.96932	0.99654

The scatter of the experimental data about the regression lines in the two figures (10 and 11) selected for demonstration indicates that the estimates obtained for the parameters are quite good. In case of a fairly incorrect estimate of N_o, the tail ends of distributions would show a stronger tendency to curve away from the regression line. Note that the correlation coefficients are - except for the 12.7 ksi stress level - a little smaller than those for the log-normal representation (Table III).

7.2.2 Upper Vertical Moment Method

Following the procedure presented in Appendix C of Ref. 19, the parameters b, N_o, and V are calculated and tabulated in Table V below.

TABLE V

PARAMETERS OF SINGLE WEIBULL DISTRIBUTION

(Upper Vertical Moment Method)

	12.7 ksi 148 spec.	13.0 ksi 148 spec.	14.0 ski 133 spec.	16.5 ksi 200 spec.
Shape parameter, b	3.135	1.819	1.438	2.138
Minimum life, N_o (mill. cycles)	0.59015	0.79284	0.31089	0.11089
Characteristic life, V (mill. cycles)	1.65184	1.38605	0.49197	0.22850
Correlation Coeffic., r	0.99649	0.99371	0.99504	0.99828

	16.5 ksi 150 spec.	16.5 ksi 350 spec.	19.0 ksi 100 spec.
Shape parameter, b	2.25439	2.19052	1.81487
Minimum life, N_o (mill.cycles)	0.138887	0.121481	0.0568477
Characteristic life, V (mill.cycles)	0.221759	0.225820	0.0735204
Correlation coeffic.,r	0.98281	0.98383	0.88723

In magnitude these parameters differ somewhat from those obtained by the classical moment method (Table IV). However, the differences are small in comparison with the large effects which small numerical variations in the upper vertical moment ($\bar{x}_r$) have on these parameters. Figure 12 shows the variations in shape of the frequency distribution functions for both methods, but only for the more significant stress levels. Note that the correlation coefficients obtained by the upper vertical moment method are in all cases, except for the 16.5 and 19 ksi stress level higher than those for the log-normal distribution and for the classical moment method. This fact is further demonstrated by Figs. 13 and 14, when compared with Figs. 10 and 11. On the other hand, a comparison of Figs. 8 and 15 demonstrates that the upper vertical moment method or, in fact, any three-parameter distribution function, does not duly represent the endurance data at high stress levels.

7.3 Truncated Log-Normal Distributions

If the endurance data at one stress level suggest a combination of two distribution functions (as e.g. in Fig. 7, dashed lines), two problems arise:

1. the problem of separating the two distribution functions, which in our case here obviously overlap,

2. to find out by what type of distribution function, either one of the two distributions can be represented best.

7.3.1 Methods of Separating

There are only a few possibilities. The simplest is to use the valley in the histograms (see Fig.4) or the jog (dashed lines) of the probability curves (in e.g., Fig.7) for obtaining a rough estimate of the point where the two distributions meet. Obviously, the jog in Fig. 7 is more realistic than the valley. However, for separating two overlapping distributions, more sophisticated methods have to be employed. One is the truncation analysis, which will be discussed subsequently, the other one is Weibull's latest method for separating components of mixed (Weibull) distributions. This will be discussed in a later paper.

7.3.2. Truncation Analysis

If for an endurance distribution the distribution is known only below or above a certain endurance (called truncation point), the distribution is said to be truncated. From the known portion of a truncated distribution the $\bar{X}$ and S^2 of the entire distribution can be estimated by Hald's method as outlined in Appendix A of Ref.19.

Imagine now that in Fig. 4, the truncation point is moved step by step from the low to the high endurance tail. Using the IBM 7090/7094-II computer, the X and S values were calculated for, in fact, almost all endurances with the exception only of the extreme tail ends of the distributions. Typical changes in mean life (X) and standard deviation (S) with increasing number of specimens in the truncated sample (n_{tr}) - the truncation point moving from left to right in Fig. 4 or Fig. 7 - are shown in Fig. 16. We see that for small numbers of specimens (samples), the calculated standard deviation for the whole sample varies rather incoherently. Logically, S should become smaller and smallest when the truncation point in Fig. 4 reaches the peak of the low (left) endurance distribution. In Fig.16, this point is indicated by the dip in the S-curve marked by the line which divides the STF (short term fatigue) from the LTF (long term fatigue) range. The subsequent rise of the S-curve indicates a larger variation (scatter) of the endurance data, which in turn suggests that beyond that lowest S value, the effect of the high (second) endurance distribution becomes visible. Ultimately, when the truncated sample number (n_{tr}) approaches that of the test sample, the standard deviation equals that calculated under the assumption that the test sample is representing a single log-normal distribution (see Fig. 16).

Starting truncation at the high endurance end and letting the truncation point move towards lower endurances results in Fig. 17, for e.g., the 13 ksi stress level. Obviously, the parameters vary in such a manner that no trend can be detected from which an indication of the extent of the low life end of the high endurance

distribution could be obtained. Equivalent plottings for the 12.7 and 14 ksi stress levels (see Ref.19) provide similar evidence. One reason may be that the endurance distributions for the 12.7 to 14 ksi stress levels do fit Weibull distribution functions better (compare correlation coefficients in Tables III and V) than log-normal ones, for which alone the demonstrated truncation analysis is applicable.

To fully demonstrate the scope of the truncation analysis, let us look at Fig. 18 plotted for the 19 ksi stress level. There is no evidence to suggest the existence of bimodality. This also holds true in principle for the 16.5 ksi stress level. If one compares this evidence with the large scatter at the lower stress levels, caused by the blending of two endurance distributions, the following model seems to emerge. It is known that as the stress level approaches the high stress (H-) region of the S-N curve, the means of the component distributions approach each other. At the same time, the high endurance distribution diminishes. A simple analysis (see Appendix A of Ref.21) shows that if the two component distribution means are finally separated by less than 2.2 times the mean standard deviation $(\sigma_1 + \sigma_2)/2$, only a single peak (mode) will show. Hence, under such conditions, the truncation analysis can no longer detect the existence of bimodality.

7.4 Parameters of the STF and LTF Component Distributions

Assuming that the "dip" in the $\bar{X}$ and S parameter curves (e.g., Fig. 15) defines the end of the range of predominance of the STF component distribution, the $\bar{X}$ at the dip is used to estimate the total number of specimens in the STF distribution by taking twice the number of specimens, which had endurances smaller than $\bar{X}$. The parameter of the STF component distributions for which the total number of specimens could be estimated in the above manner are shown in Table VI.

TABLE VI

PARAMETERS OF THE LOG-NORMAL STF COMPONENT DISTRIBUTION

	12.7 ksi	13.0 ksi	14.0 ksi	16.5 ksi
Mean life, $\bar{X}$	5.9726	6.0080	5.5715	5.1868
Stand. deviation, s	0.04032	0.03925	0.03835	0.04750
No. of specimens from truncation	-	42	4	38
Histogram	14	54	44	44
Correlation,coeffic, r	—	0.98419	0.98088	0.9894

Note that for $\bar{X} = 5.57$ at 14 ksi, the number of specimens of smaller endurance than log N = 5.57 is 22, which if doubled confirms the total number of 44 specimens in that STF component distribution. However, total numbers (see Table VI) for other stress levels support the fact that this method of separation of the STF from the LTF endurance distribution is, at its best, approximate. This fact

is further emphasized when the parameters for the LTF component distribution are calculated. Taking account of the fact that Weibull distribution functions fitted the high endurance data better than log-normal distributions, the parameters listed in Table VII are Weibull parameters.

TABLE VII

PARAMETERS OF THE WEIBULL LTF COMPONENT DISTRIBUTION

Shape parameter, b	1.827	1.444	1.608	1.625
Min. life, N_o (mill. cycles)	1.084	1.086	0.417	0.158
Characteristic life, V (mill.cycles)	1.648	1.486	0.541	0.238
Mean of N, $\bar{N}$ (mill.cycles)	1.607	1.447	0.538	0.226
Mean of log (N), $\bar{x}$	6.1994	6.1543	5.7241	5.3462
Stand.dev.of log (N)	0.07429	0.07203	0.07508	0.08440
Correl.coeff., r	0.99837	0.98527	0.99096	0.99584
Estim.No. of specimens in LTF component distribution (No.of specimens having $N \geq N_o$)	136	107	84	165
Percent LTF of total	90.6	71.0	62.4	82.5

7.5 Identification of the STF and LTF Component Distribution Functions

Summarizing the observations presented in the foregoing sections we can, using the correlation coefficient as the criterion for goodness of fit(for justification of this choice, see Sec. 7.6) tabulate the evidence as shown below in Table VIII.

TABLE VIII: GOODNESS OF FIT

BEST FIT (x)		LOG-NORMAL	or	WEIBULL DISTRIBUTION (UPP. VERTICAL MOMENT)
Stress Level	No.of Spec.			
12.7	148	148*Fig.7		x 148*Fig.13
13	148	148 Fig.7		x 148
14	133	133 Fig.7		x 133 Fig.14
16.5	200	200 Fig.7		x 200
16.5	150	x 150		150
16.5	350	x 350		350
19.0	100	x 100 Fig.8		100 Fig.15
12.7	148	14*	LTF	x
13	148	STF x 54 Fig.19	LTF	x 107*
14	133	STF x 44 Fig.19	LTF	x 84 Fig.20
16.5	200	STF x 44 Fig.19	LTF	x 173
16.5	150	No bimodality		
16.5	350	No bimodality		
19	100	No bimodality		

* Indicates number of specimens in distribution.

Whereas proof that endurance data fit either single log-normal or Weibull distribution functions best, was given earlier in typical plottings such as Figs. 7, 8, 13, 14 and 15, the following figures demonstrate the goodness of fit of the STF and LTF component endurance data. In Fig. 19, the specimen lines of the 13, 14 and 16.5 ksi STF components are plotted on log-normal probability paper, taking the total cumulative probability for each STF mode equal to unity. These plots show that the low endurance (STF) components are well represented by a log-normal distribution. Figure 20 shows the high endurance (LTF) component for the 14 ksi case plotted as Weibull probabilities (upper vertical moment method) for comparison. The parameters for N_o and r are given in Table VII and in Fig.20. The endurances used for the LTF component are all those greater than N_o. As to Fig.20, it is obvious that the fit is not as good as it is in the single Weibull (upper vertical moment) plot of Fig.14.

The endurance scatter ranges for both the STF and LTF component modes and their mean values, are presented in Fig. 21. The standard deviations for the STF and LTF modes and the single distribution are plotted in Fig.22. It is seen that the standard deviation of the STF and LTF modes are separated by a factor of two. This in itself can thus far be considered the most convincing evidence that the endurance data represent a single distribution with two modes, or what is called a bimodal distribution.

7.6 Correlation Coefficient and Goodness of Fit

Statistical independence of the test data is an essential requirement for the usefulness of correlation coefficient for goodness of fit comparisons. Since the endurance distributions in question are not solely normal distributions - to which the X^2-test could be best applied - it was decided to use the correlation coefficient in lack of any other method we know of, which can be applied to both normal and Weibull distributions. It should be emphasized that we are not only interested in knowing how well a specific distribution fits the endurance data, but also in knowing which distribution fits the data best. The correlation coefficient, calculated for the straight lines shown on the probability paper plots of, e.g., Figs. 7 and 14, as a common basis for comparing the goodness of fit seems to fulfill this purpose best.

7.7 The Mathematical Dissection Method

At the higher stress levels, the means of the component distributions approach each other and the LTF component diminishes. Under these conditions, the truncation analysis become ineffective in detecting the existence of bimodality (see Appendix A of Ref. 21). Therefore the mathematical dissection method, as outlined in Appendix B of Ref. 21, was applied to the 16.5 and 19 ksi test endurances.

To simplify the analysis, the bimodal distribution (STF and LTF) was assumed to consist of two log-normal distributions (instead of log-normal and Weibull) and it was on this basis that

the parameters of these two distributions were calculated. They are shown in Table IX below.

TABLE IX

PARAMETERS OF MATHEMATICAL DISSECTION METHOD

	16.5 ksi 150 specimens	16.5 ksi 350 speci.	19.0 ksi 100 speci.
STF Component, h_1	0.999854	0.999774	0.997580
Mean of log(N), m_1	5.320897	5.320587	4.850606
Standard deviation, s_1	0.074330	0.088239	0.047027
LTF Component, h_2	0.000145	0.000225	0.002419
Mean of log (N), m_2	5.312835	5.298581	5.272022
Standard deviation, s_2	2.028144	1.260850	0.145477

The parameters suggest that there is only a single distribution at both stress levels, as indicated by the practically insignificant values for h_2, expressing the proportion of the LTF component present.

7.8 Concluding Remarks

On the basis of the statistical analysis presented thus far, the following evidence for bimodality of the OFHC copper endurance distributions emerges:

1. the apparent bimodality in the endurance histograms for the low stress levels (see e.g. Fig.5)

2. the significantly and consistently different values for the standard deviations of the STF and LTF modes at the lower stress levels (see Fig.22)

3. the consistent variations in the STF parameters obtained by the maximum likelihood truncation method.

VIII. ANALYSIS OF THE ENDURANCES OF BLOOMER AND ROYLANCE

Bloomer and Roylance (Ref.22) tested 973 notched aluminum (B.26 S-WP: 2024-ST) specimens in four rotating bending cantilever type machines at a nominal stress of about 16.8 ksi. Figure 23 shows a typical histogram which suggests a fair amount of random disturbances and irregularities in the sample. This observation is further emphasized by the results of the truncation analysis, which was also applied to the test data of Ref. 21. Whereas one of the four samples seems to indicate the existence of two distributions, the others do not. Figure 24 is typical for the latter and Fig. 25 shows the same data (of machine No.3) plotted on log-normal probability paper. The correlation coefficients for all machines demonstrate that the log-normal distribution does not fit the test data too well. For comparison, Fig. 26 presents a plot of the same data

but now on extreme value probability paper, with the straight line fitted by the upper vertical moment method. Since no regression analysis could be carried out in this case (see Ref. 21 for reasons), correlation coefficients could not be used to determine the relative goodness of fit of the log-normal and log-Weibull distributions. However, the parameters calculated for both types of distribution are given in Table X below.

TABLE X

BLOOMER AND ROYLANCE TEST DATA (REFERENCE 22)

(A) PARAMETERS OF SINGLE LOG-NORMAL DISTRIBUTION

Machine No.	1	2	3	4
Number of Specimens	243	255	245	230
Mean of log (N), $\bar{X}$	5.95902	5.94342	5.97992	5.97745
Standard deviation, s	0.177530	0.164388	0.189107	0.190898
Correlation coeff., r	0.93047	0.94431	0.88778	0.91626

(B) PARAMETERS OF SINGLE LOG-WEIBULL DISTRIBUTION (UPPER VERTICAL MOMENT METHOD)

Machine No.	1	2	3	4
Number of Specimens	243	255	245	230
Shape parameter, b	1.54682	1.76714	1.45728	1.29897
Minimum life, log N_o	5.70737	5.68136	5.74261	5.74781
Characteristic life, log V	5.98883	5.97763	6.00701	5.99812

The mathematical dissection method, applied to these results also, did not converge, possibly because of the irregularities in the samples already mentioned above in connection with the histograms. For further details, see Ref.21.

IX. METALLOGRAPHIC EXAMINATION OF FATIGUED SPECIMENS

The purpose of this examination was to see whether specimens from either the STF or LTF component distribution can be perhaps microstructurally differentiated. Obviously, the probability of finding any differences must be the greatest if specimens are taken from the low and high endurance tail ends (see log N < 5.5 and log N > 5.9 in e.g., Fig.4) of the endurance distribution for a given stress level. It was speculated that, based on the evidence presented in Fig.27, Wood's H and F fatigue mechanisms might be found to be the cause for the observed bimodality, ie., the failure of specimens in eitherthe STF or LTF mode.

9.1 Examination of Fatigued Specimens

For details about routine pre-metallographic testing, specimen sectioning and preparation, X-ray tests, electro-polishing and etching, examination of the specimen surface before and after fatigue, etc., see Ref. 20.

9.1.1 The Examination Results

Each one of the three ranges, H, F, and S has, according to Wood (Ref.5), distinctive microstructural characteristics such as, for instance, sub-grain (cell) formation and grain boundary cracking in the H-range or distorted slip zones and slip zone microcracks in the F-range. It should be noted, however, that in none of these stress (strain) ranges, the distinctive microstructural characteristics of any such range prevail exclusively. They only predominate and in the transition region between, e.g., the H and F range, the microstructural characteristics of both ranges coexist.

An estimation of the percentage share of each range was attempted under the microscope by counting the number of grains showing characteristic H, F and S fatigue damage. This method was sensitive enough to detect the changes in percentage fractions of the three ranges from one to another of the stress amplitudes tested. However, it was not sensitive enough to distinguish between the STF and LTF distribution specimens at one and the same stress level. The percentage estimates obtained in this way are shown in Table XI and are compared with the number of specimens (in percent) in the STF and LTF distributions.

TABLE XI

PERCENTAGES OF H, F AND S FATIGUED SPECIMENS IN COMPARISON WITH STF AND LTF PERCENTAGE IN BIMODAL DISTRIBUTIONS

Stress amplitude	Microstructures		Test Results (Refs.20 & 21)	
	Percentage of			
(ksi)	H	F and S	STF	LTF
± 10.0	-	≈100	-	≈100
± 12.7	5	95	≈5	95
± 13.0	30	70	37	63
± 14.0	30	70	33	67
± 16.5	40	60	<22	>78
± 19.0	60	40	-	≈100

The percentages of the H and F range microstructure at a given stress amplitude reasonably agree with the percentages of the apparent STF and LTF fractions of the statistical bimodal endurance distributions. However, an attempt to distinguish by the same method between the STF and LTF specimens, taken from the endurance tail ends of one bimodal distribution failed to show any significant microstructural differences. Also electron microscopy

did not reveal characteristic differences on which an unambiguous separation of STF or LTF fatigued specimens, fatigued at one and the same stress level could be based.

Further details, demonstrating the transition from F to H-range fatigue damage in typical photomicrographs and X-ray back reflection patterns are given in Refs. 20 and 21.

For completeness, Table XII is added to show the macro- and microhardness test values of specimens fatigued at the stress levels shown.

TABLE XII

MACRO- AND MICROHARDNESS TEST VALUES OF FATIGUED SPECIMENS

Stress amplitude (ksi)	Microhardness (D.P.N.) H grain	F grain	Macrohardness (D.P.N.)
± 12.7	73.0	53.5	76.5
± 13.0	80.0	61.2	79.0
± 14.0	80.9	53.5	73.5
± 16.5	81.3	55.9	73.5

X. HYPOTHESIS FROM TEST RESULTS

The evidence presented in Finney's review strongly supports his statement that "no attempt is made in this report to detail the actual fatigue mechanisms which may be involved; instead it is simply suggested that the discontinuity arises from a multiplicity of fatigue mechanisms and that more basic studies are necessary for a fuller explanation".

Our test results do not supply the information for this fuller (final) explanation. However, they indicate that the shape of the bumps or discontinuity is strongly affected by the degree of overlap of the observed endurance distributions, which in turn are indicative of at least two basic fatigue mechanisms. In principle, one could perhaps advance the hypothesis that going from single crystals to polycrystaline and alloyed materials, the endurance distributions at stress level at the lower knee change from single and bimodal to a two endurance distribution pattern. This hypothesis is demonstrated in Fig. 28 and published experimental evidence (Refs. 2, 3 and 23) seems to support it.

XI. CONCLUSIONS

The main results of this study can be summarized as follows:-

1) the two endurance distributions, so clearly, observed with alloys, could not be confirmed for polycrystalline (OFHC) copper.

Instead,

2) at stress levels around the lower knee the existence of two (or perhaps three) modes (bimodality) is apparent,

3) at stress levels well above the knee, endurance distributions seem to become single log-normal, below the knee extremal,

4) the bimodality seems to be caused by a transition of predominance from one to another fatigue mechanism (e.g. Wood's F to H range transition),

5) Prof. W. Weibull is at present applying his latest computerized methods for separating bimodal distributions. A co-authored paper is pending,

6) Finney's statement (see his conc usions) that the bump or discontinuity phenomenon "is influenced by a number of factors including the metallurgical condition of the material, type of fatigue test, severity of stress concentration, frequency of cycling, test environment and temperature", etc., may be supplemented perhaps by the observation of our tests that the degree of overlap of the detected endurance distributions (single, bimodal or double) seems to depend primarily upon the microstructural characteristics (single crystal, polycrystal or alloyed) of the tested material.

REFERENCES

1. Finney, J. M. — "A Review of the Discontinuity or Hump Phenomenon in Fatigue S/N Curves: Theories and Further Results". Report SM 314, March 1967.

2. Swanson, S. R. — "A Two-Distribution Interpretation of Fatigue S-N Data". Canadian Aeronautical Journal, Vol.6, No.6, June 1960.

3. Cicci, F. — "An Investigation of the Statistical Distribution of Constant Amplitude Fatigue Endurances for a Maraging Steel". UTIAS Tech.Note No.73, July, 1964.

4. Wood, W. A. — "Some Basic Studies of Fatigue in Metals". Published Jointly by Technology Press and John Wiley & Sons, 1959.

5. Wood, W. A. — "Experimental Approach to Basic Study of Fatigue". Inst. for the Study of Fatigue and Reliability, Report No.24, Columbia University, August, 1965.

6. Frost, N. E. — "Differences Between High-and Low-Stress Fatigue". Nature, Vol. 192, 1961.

7. Dolan, T. J. — "Basic Research in Fatigue of Metals". ASTM Bulletin 240, Research Sub-Committee, Committee E-9, September, 1959.

8. Swanson, S. R. — "Systematic Axial Load Fatigue Tests Using Unnotched Aluminum Alloy 2024-T4 Extruded Bar Specimens". UTIAS Tech. Note No. 35, May, 1960.

9. Swanson, S. R. — "An Investigation of the Fatigue of Aluminum Alloy Due to Random Loading". UTIAS Report No.84, February, 1963.

10. Freudenthal, A. M. — "Fatigue of Materials and Structures Under Random Loading". Page 129, WADC TR-676, March, 1961.

11. Lazan, B. J. — "Damping and Resonant Fatigue Behaviour of Materials". Page 90, International Conference on Fatigue of Metals, New York and London, 1956.

12. D' Amato, R. — "A Study of the Strain Hardening and Cumulative Damage Behaviour of 2024-T4 Aluminum Alloy in the Low-Cycle Fatigue Range". WADDTR 60-175, April, 1960.

13. Porter, J.
Levy, J. C.
"The Fatigue Curves of Copper". Journal of the Institute of Metals, Vol. 89, 1960-61.

14. Wild, M.
"Joint International Conference on Creep". New York, 25-29th August, 1963. Vol.2, Discussions Arising from Papers, Published in Vol. 1.

15. Couts, W. H. Jr.,
Freeman, J. W.
"Notch Rupture Behaviour as Influenced by Specimen Size and Preparation". Paper Annual Meeting of the ASME,December,1961.

16. Gumbel, E. S.
Freudenthal, A. M.
"Distribution Functions for the Prediction of Fatigue Life and Fatigue Strength", p. 262, International Conference on Fatigue of Metals, New York and London, 1956.

17.
International Conference on Fatigue of Metals, New York and London, 1956.

18. Keys, R. D.
Schwarzberg, F. R.
"Techniques from Axial Fatigue Testing of Sheet Materials Down to - 423°F. Paper presented at the 66th. Annual Meeting, ASTM, June, 1963.

19. Haagensen, P. J.
"Statistical Aspects of Coexisting Fatigue Failure Mechanisms in OFHC Copper". UTIAS Tech. Note No.112, June, 1967.

20. Muggeridge, D. B.
"An Attempt to Correlate Bimodal Fatigue Endurance Distributions in OFHC Copper with Wood's H, F and S Ranges". UTIAS Tech. Note No. 111, June, 1967.

21. Ravindran,R.
"Statistical and Metallographic Aspects of Fatigue Failure Mechanisms in Metals". UTIAS Tech.Note NO.123, February,1968.

22. Bloomer, N. T.
"A Large Scale Fatigue Test of Aluminum Specimens". The Aeronautical Quarterly, Vol. XVI, November, 1965.

23. Nine, H.D.
Bendler, H. M.
"Effect of Strain Amplitude on Fatigue in Copper Single Crystals". ACTA Metallurgical, Vol. 12, August, 1964.

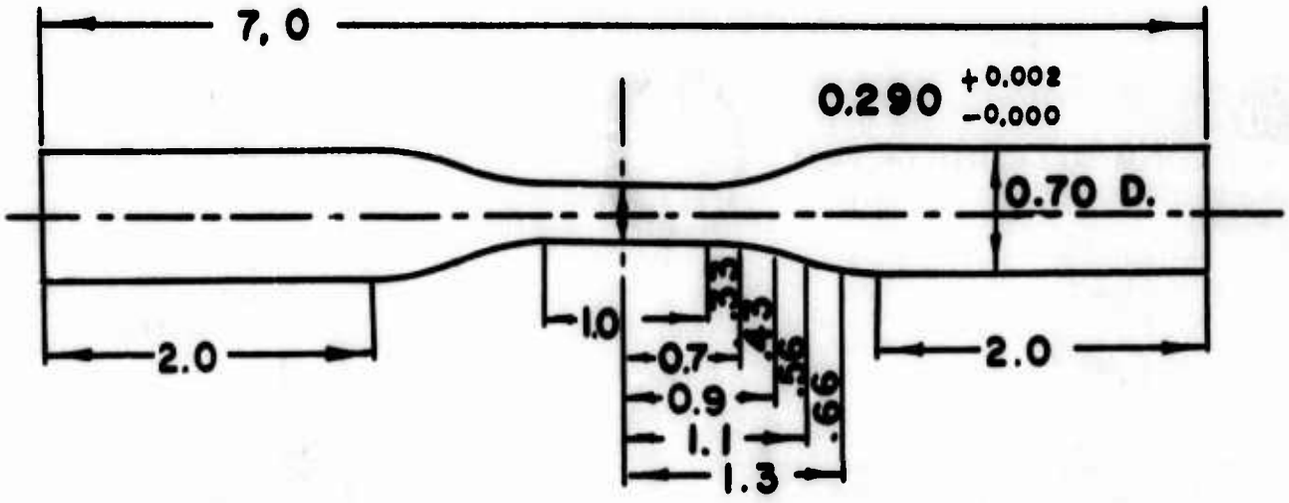

FIG. 1 THE COPPER (O.F.H.C.) FATIGUE SPECIMEN.

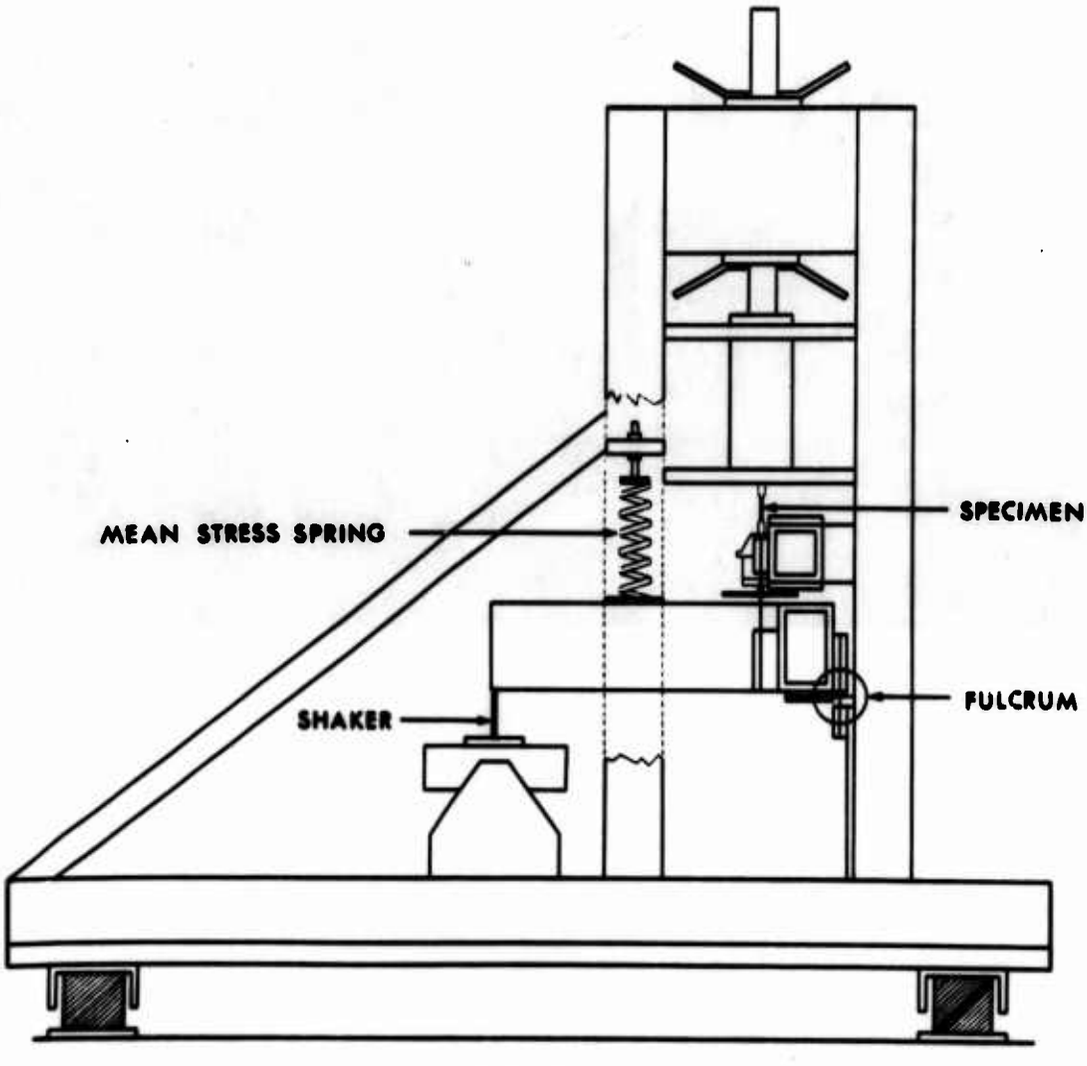

FIG. 2 (b) SCHEMATIC LAYOUT OF FATIGUE TESTING MACHINE

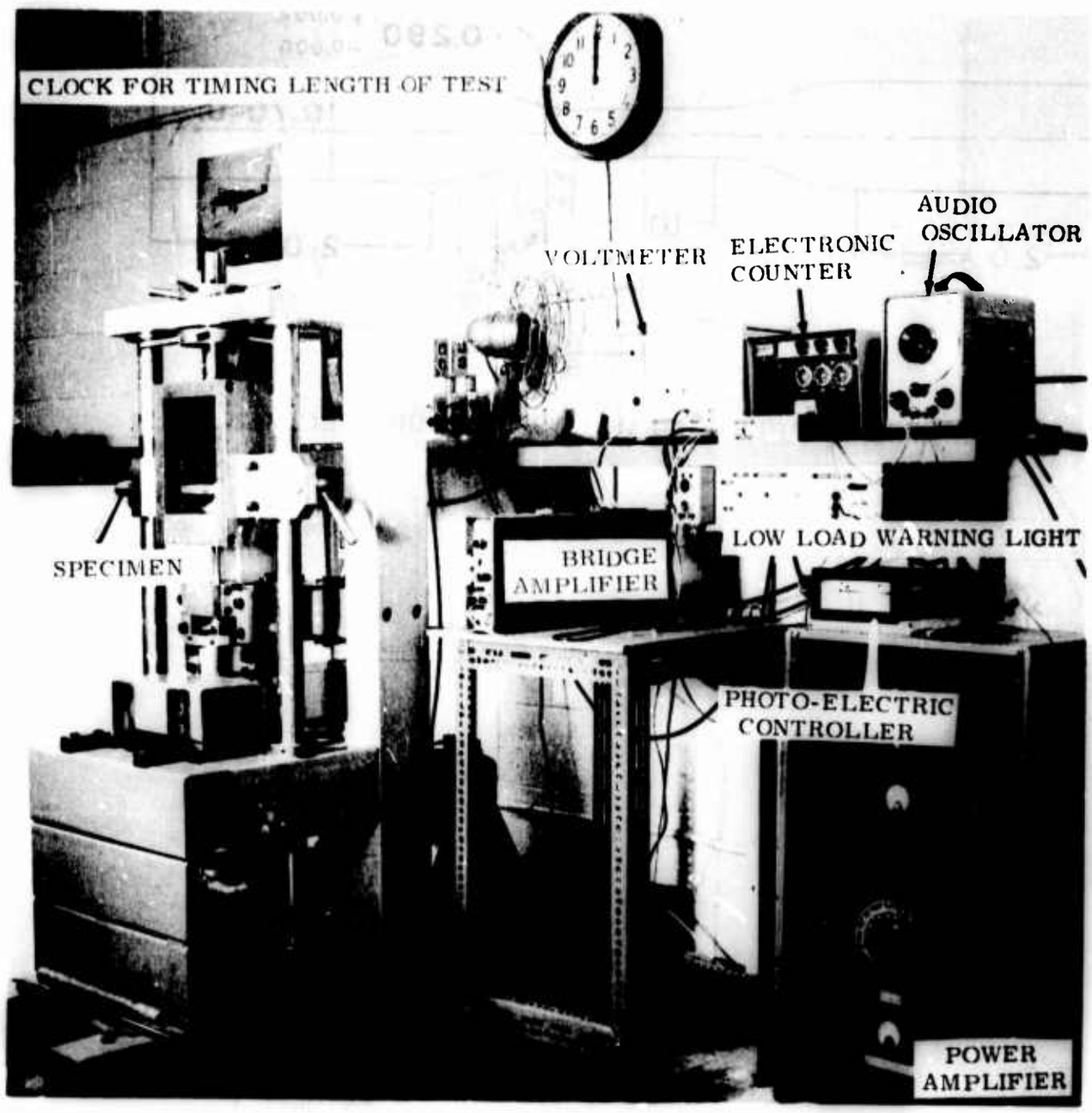

FIG-2(a). GENERAL ARRANGEMENT OF FATIGUE MACHINE AND INSTRUMENTS.

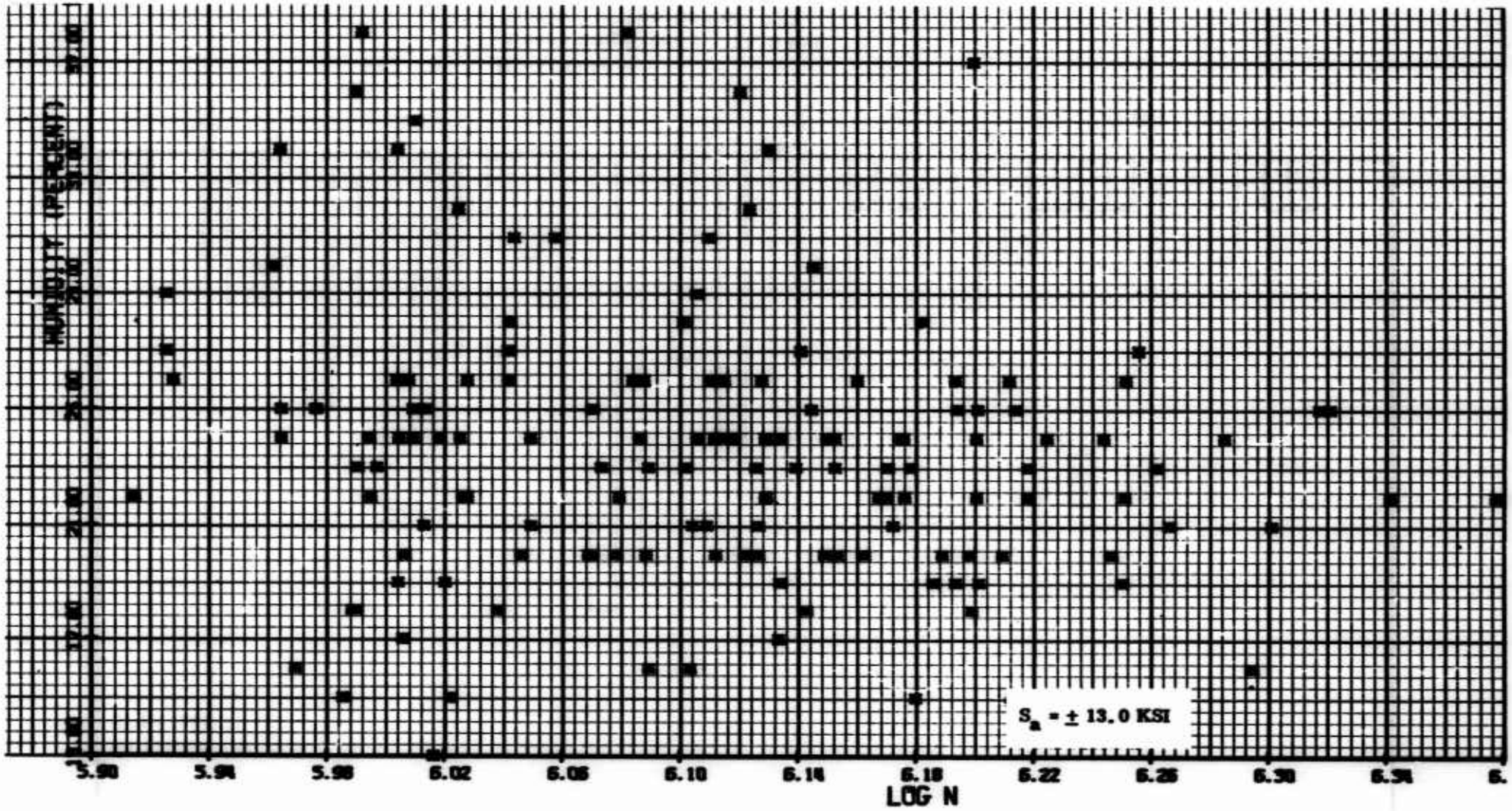

FIG. 3 HUMIDITY VS. LOG N

TOP

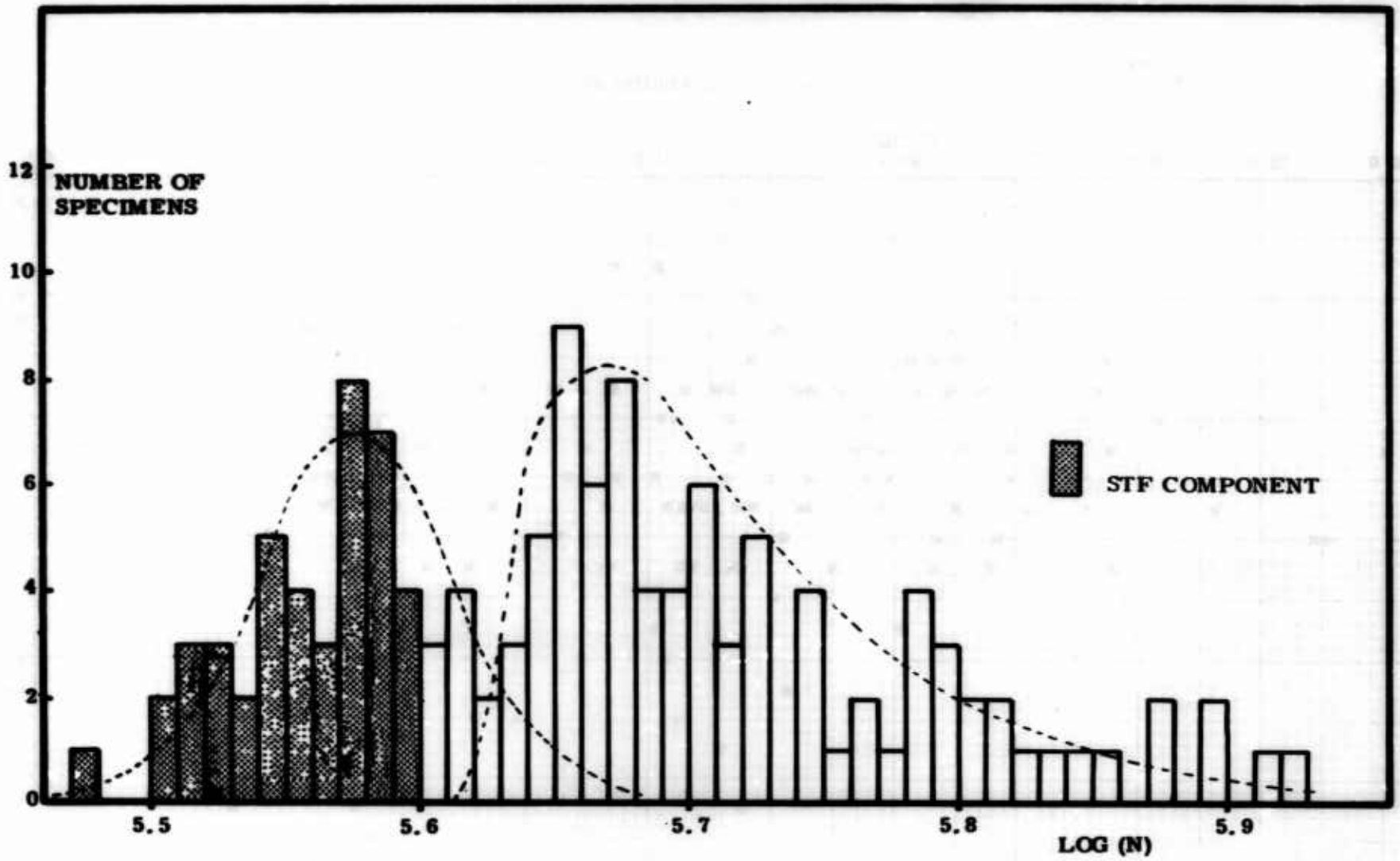

FIG. 4 HISTOGRAM
Stress amplitude : ± 14.0 ksi
Number of specimens : 133
Class length : 0.01 log(N)

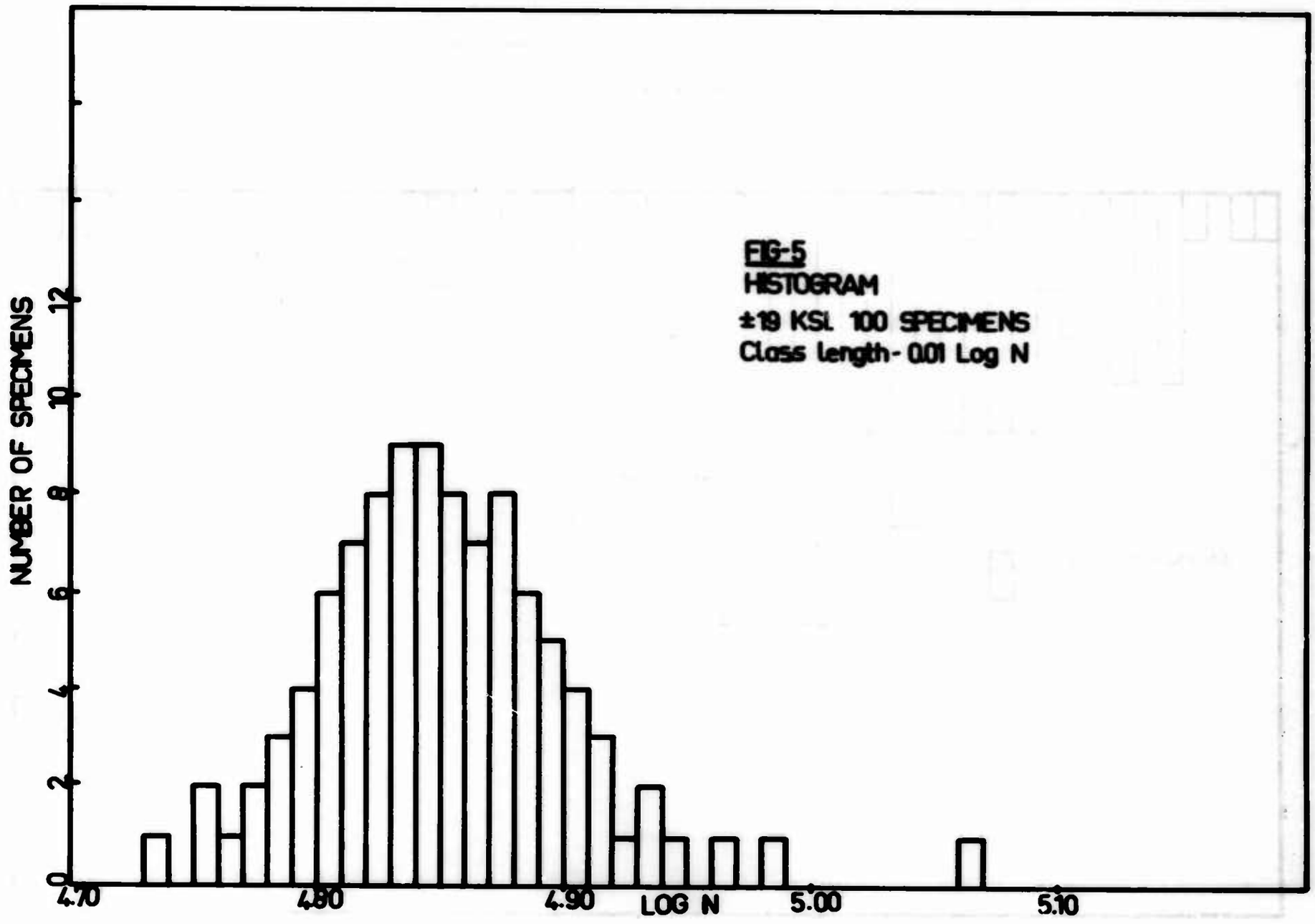
FIG-5
HISTOGRAM
±19 KSL 100 SPECIMENS
Class length- 0.01 Log N
NUMBER OF SPECIMENS
0
2
4
6
8
10
12
4.70
4.80
4.90
LOG N
5.00
5.10

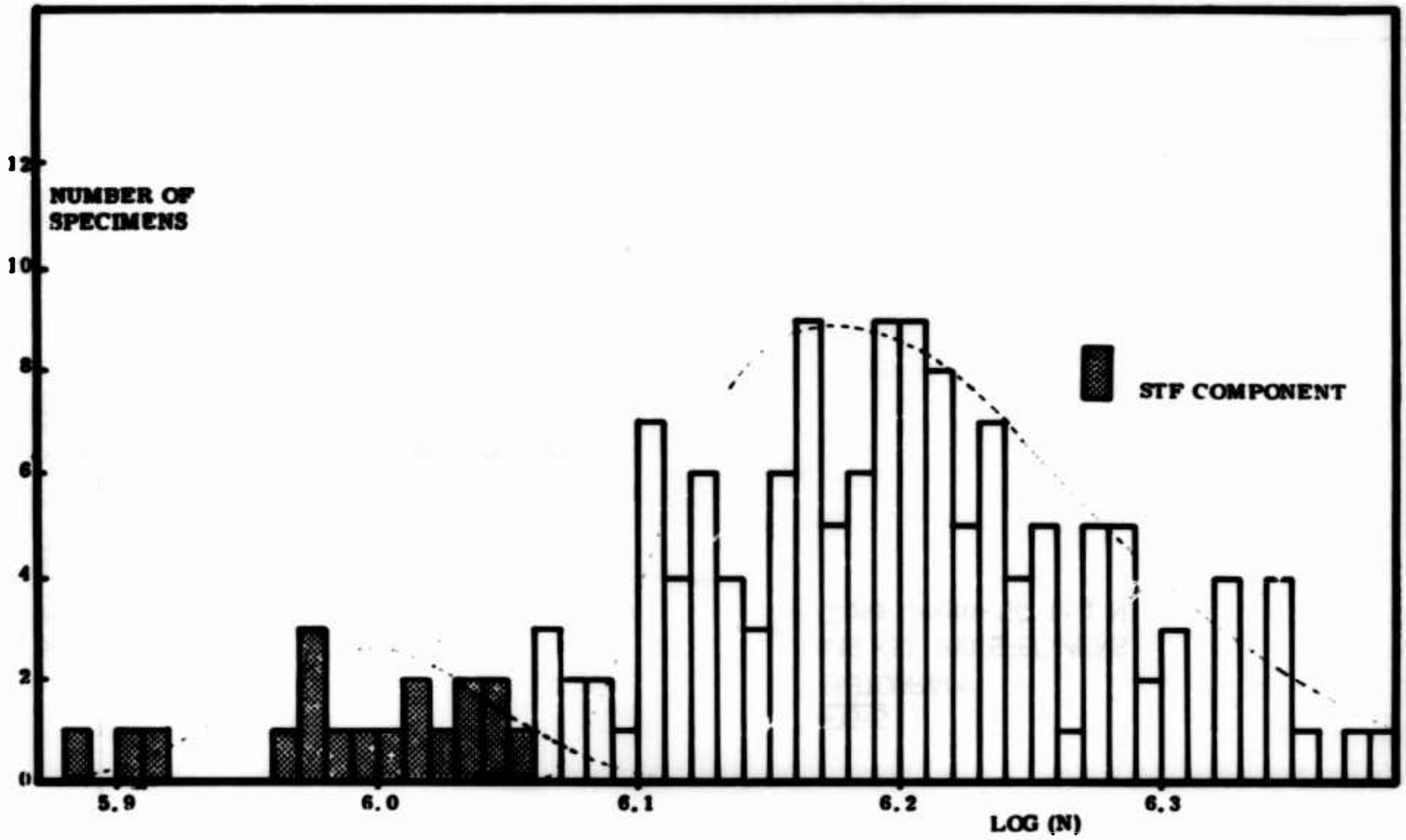

FIG. 6 HISTOGRAM
Stress amplitude : ± 12.7 ksi
Number of specimens : 150
Class length : 0.01 log(N)

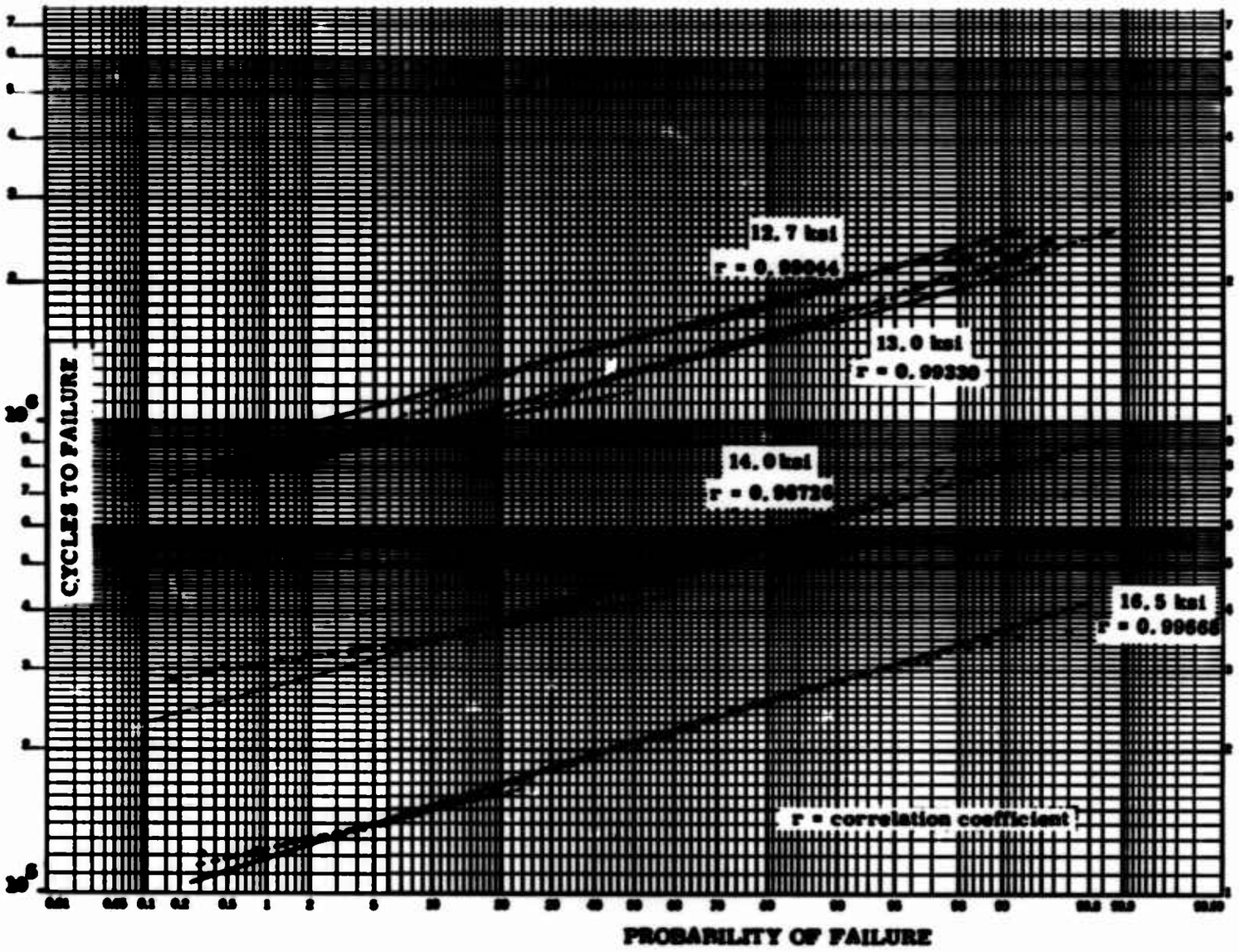

FIG. 7 LOG-NORMAL PROBABILITY PLOT, SINGLE DISTRIBUTION

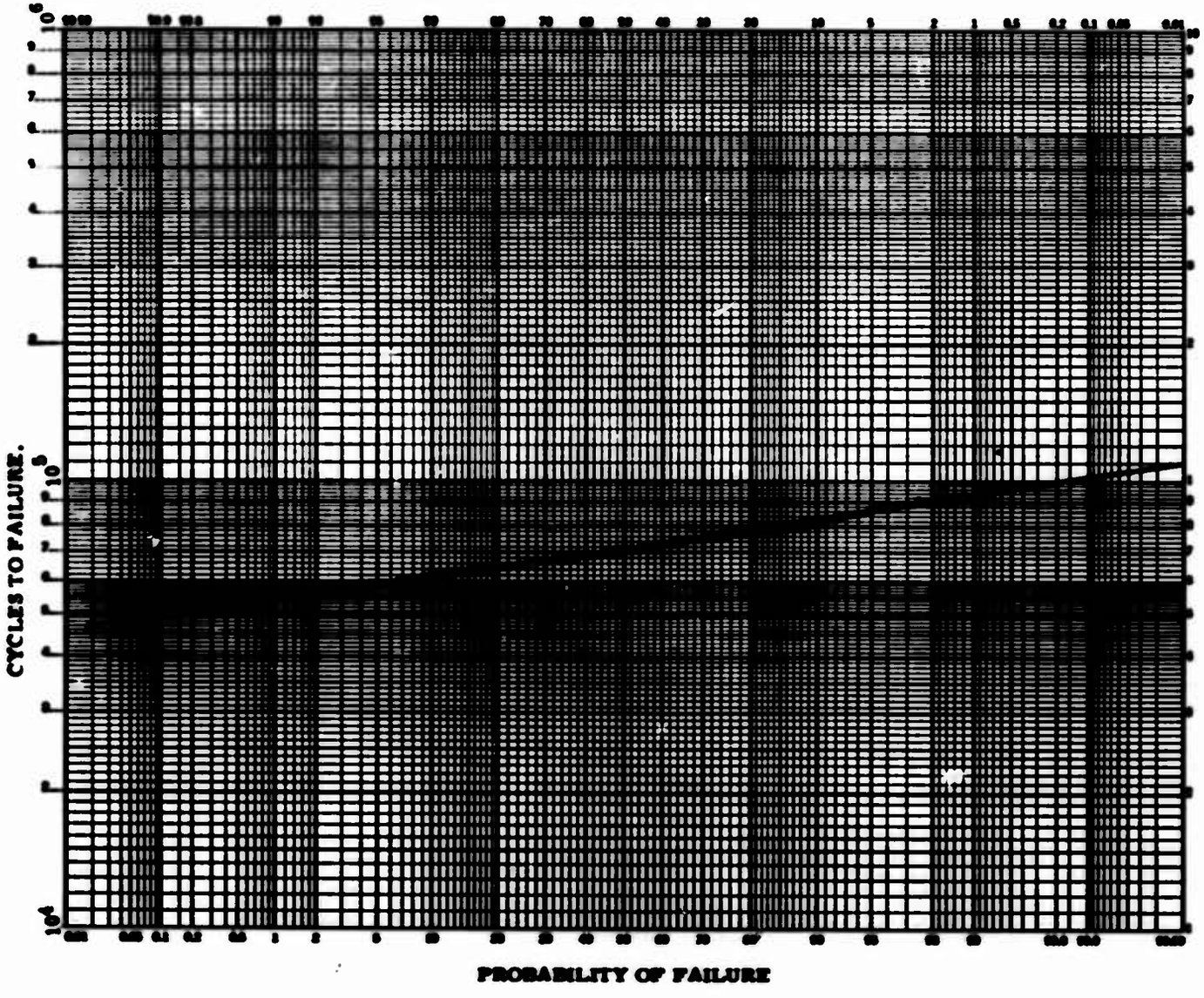

FIG. 8 LOG-NORMAL PROBABILITY PLOT. SINGLE DISTRIBUTION. 19.0 KSI, 100 SPECIMENS, r=0.97806.

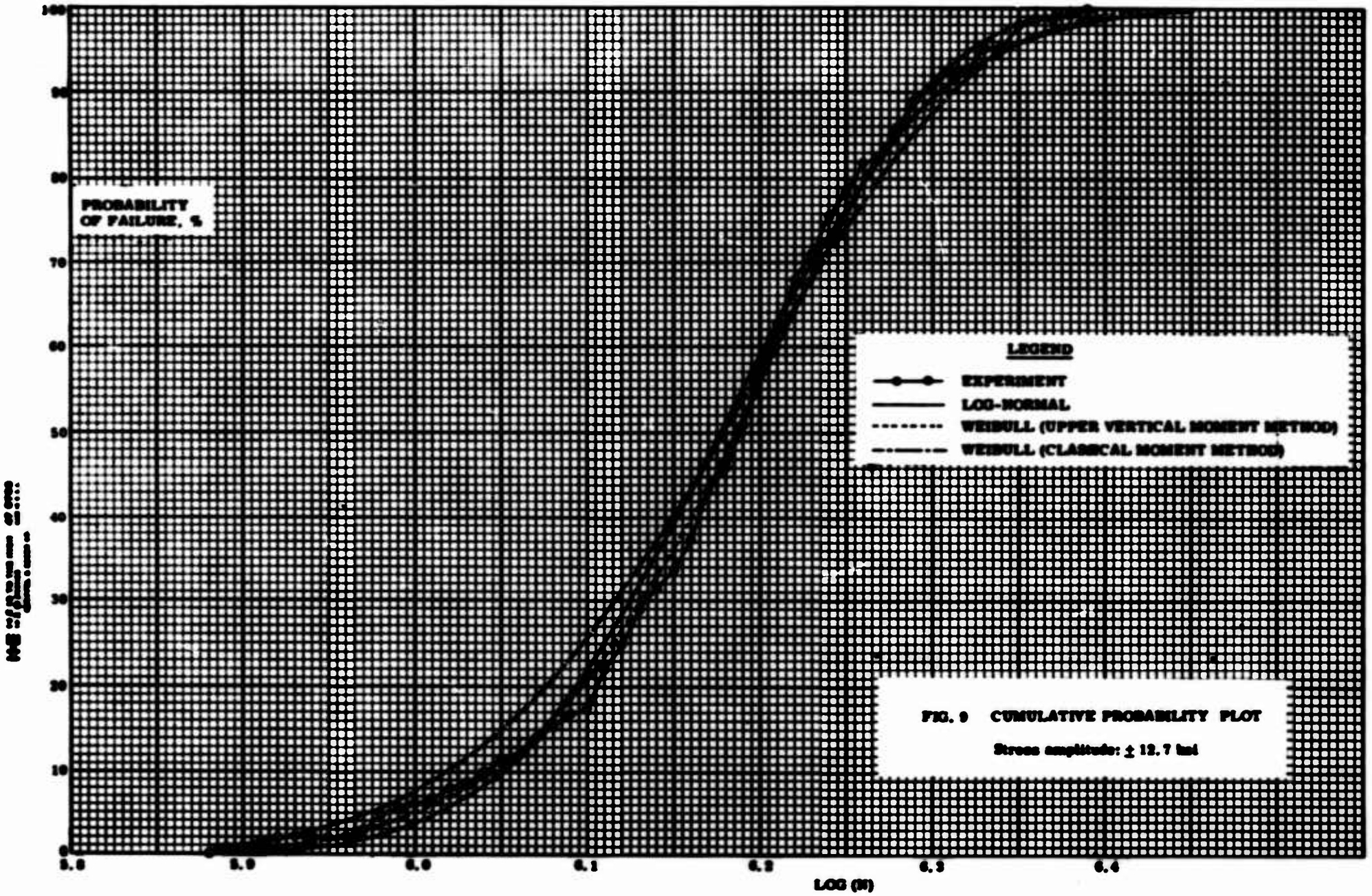

FIG. 9 CUMULATIVE PROBABILITY PLOT

Stress amplitude: ± 12.7 ksi

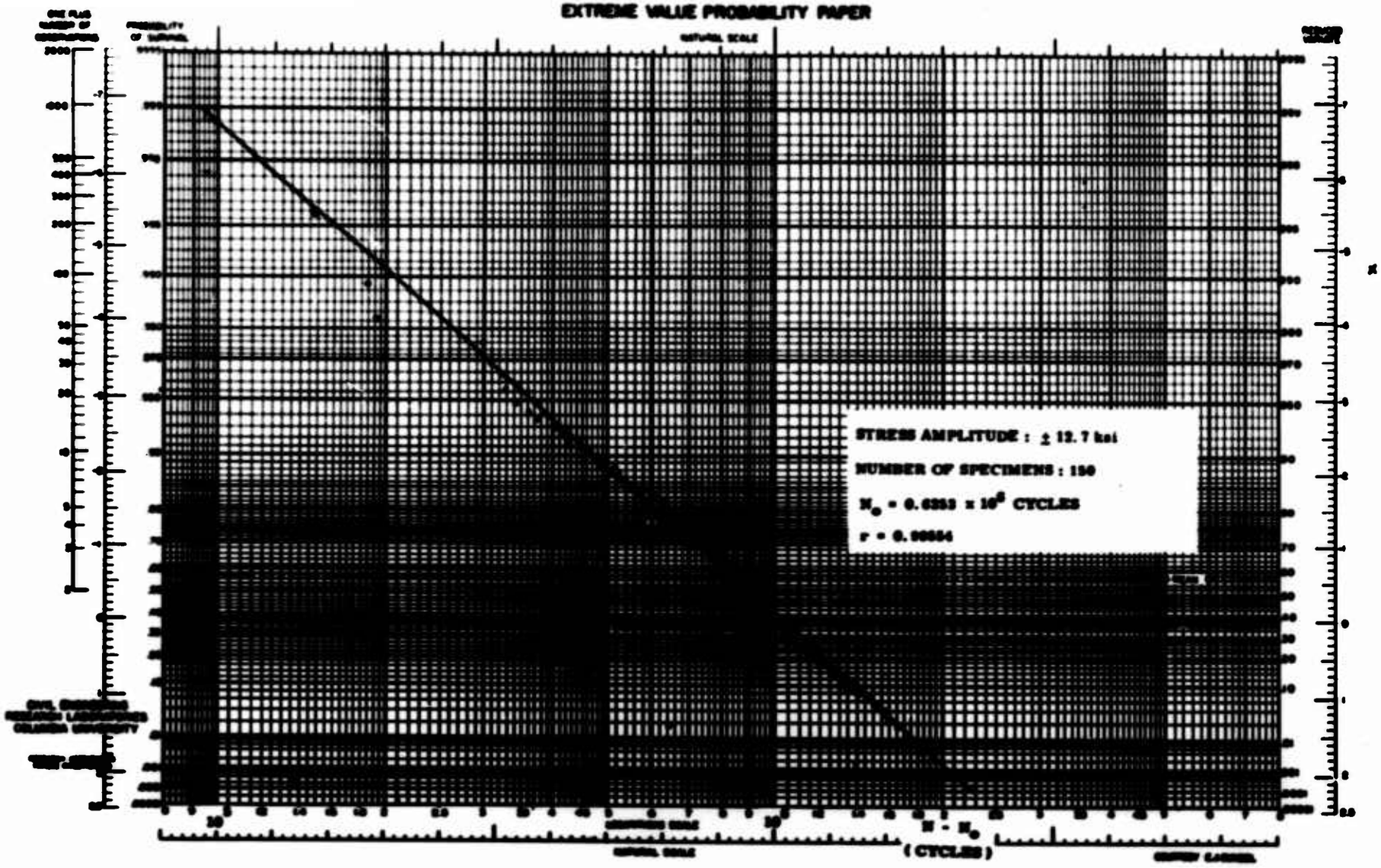

FIG. 10 WEIBULL PROBABILITY PLOT, SINGLE DISTRIBUTION. PARAMETERS CALCULATED BY THE CLASSICAL MOMENT METHOD.

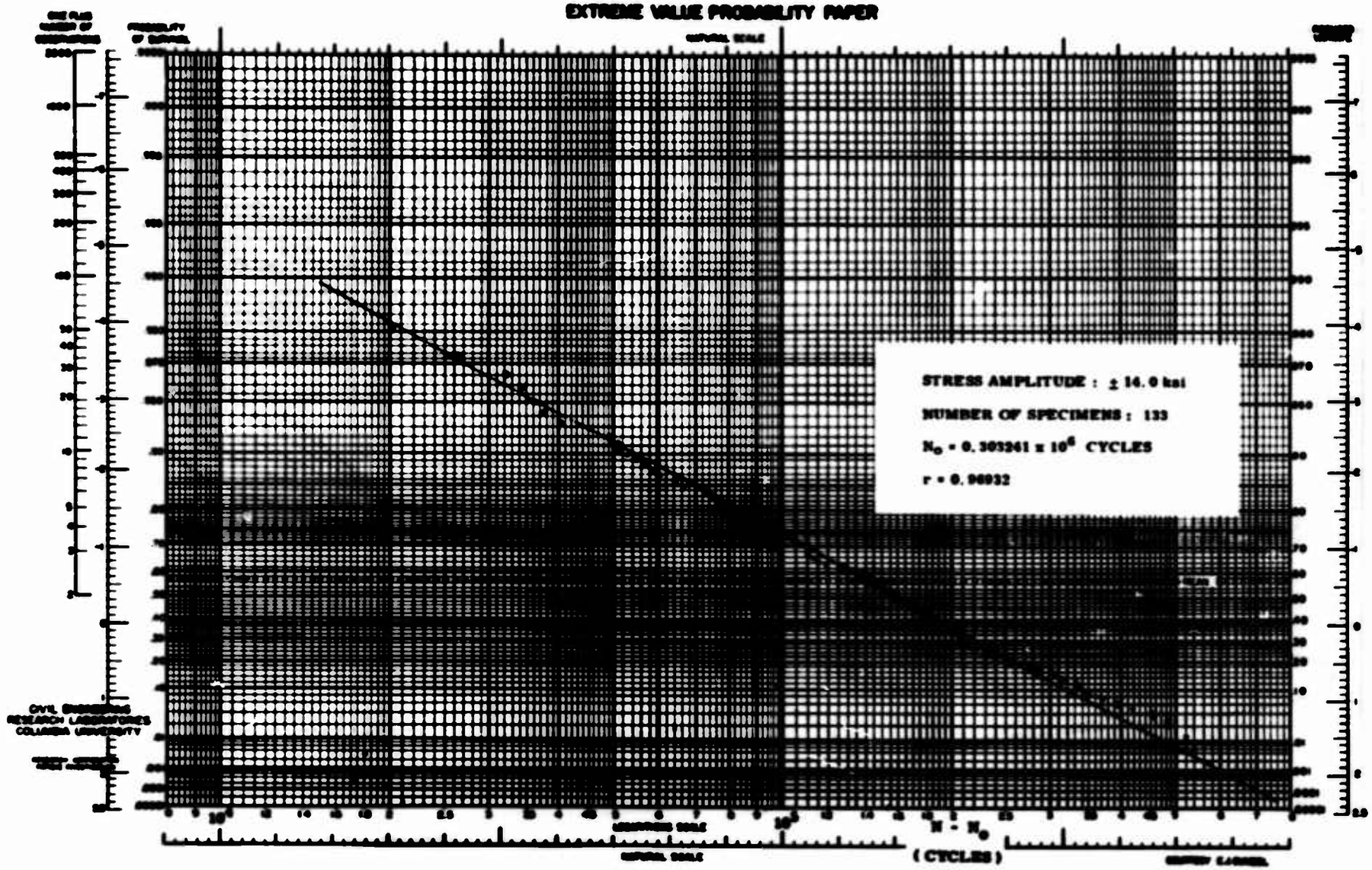

FIG. 11 WEIBULL PROBABILITY PLOT, SINGLE DISTRIBUTION. PARAMETERS CALCULATED BY THE CLASSICAL MOMENT METHOD.

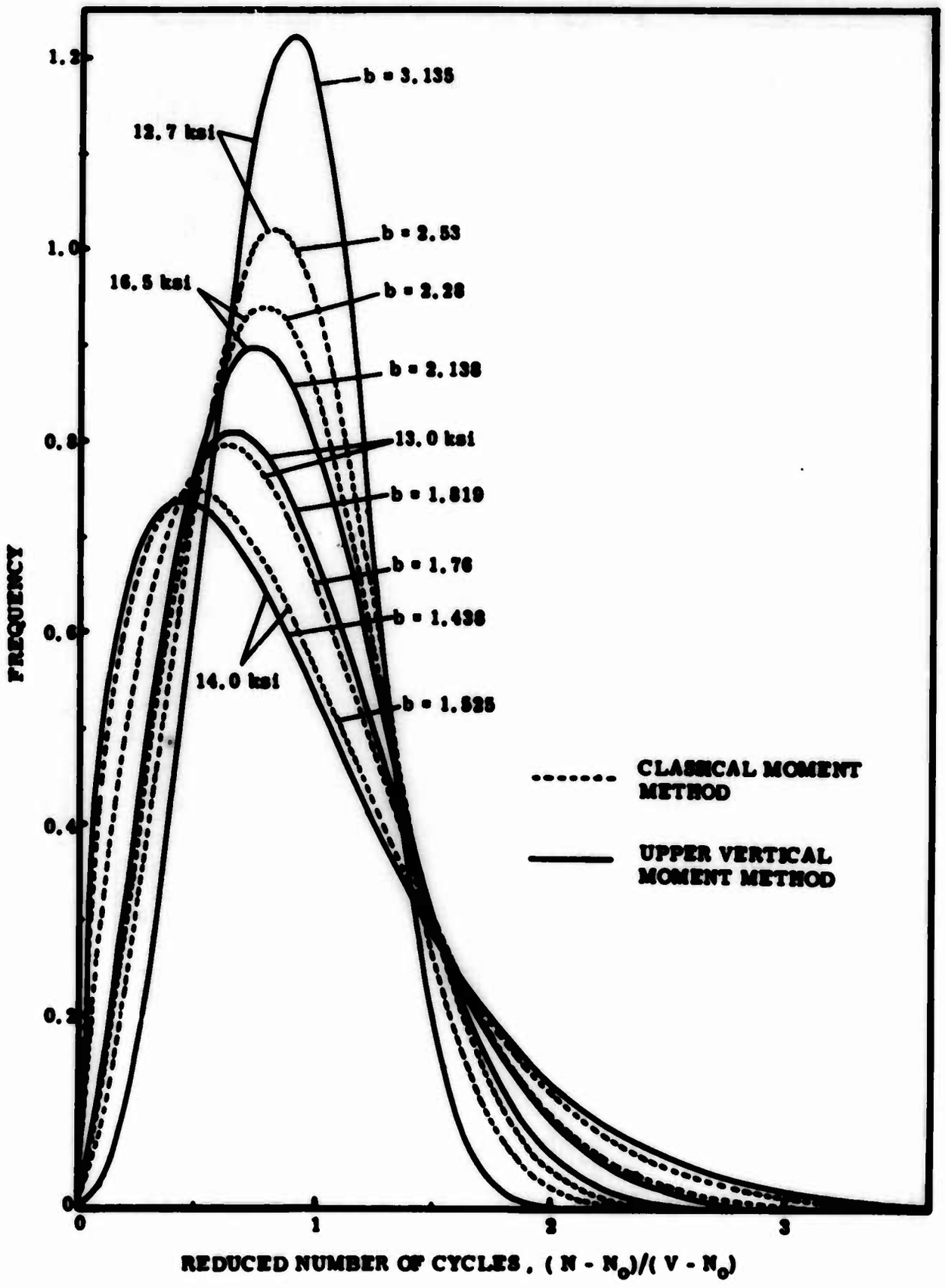

FIGURE 12 WEIBULL FREQUENCY DISTRIBUTION CURVES

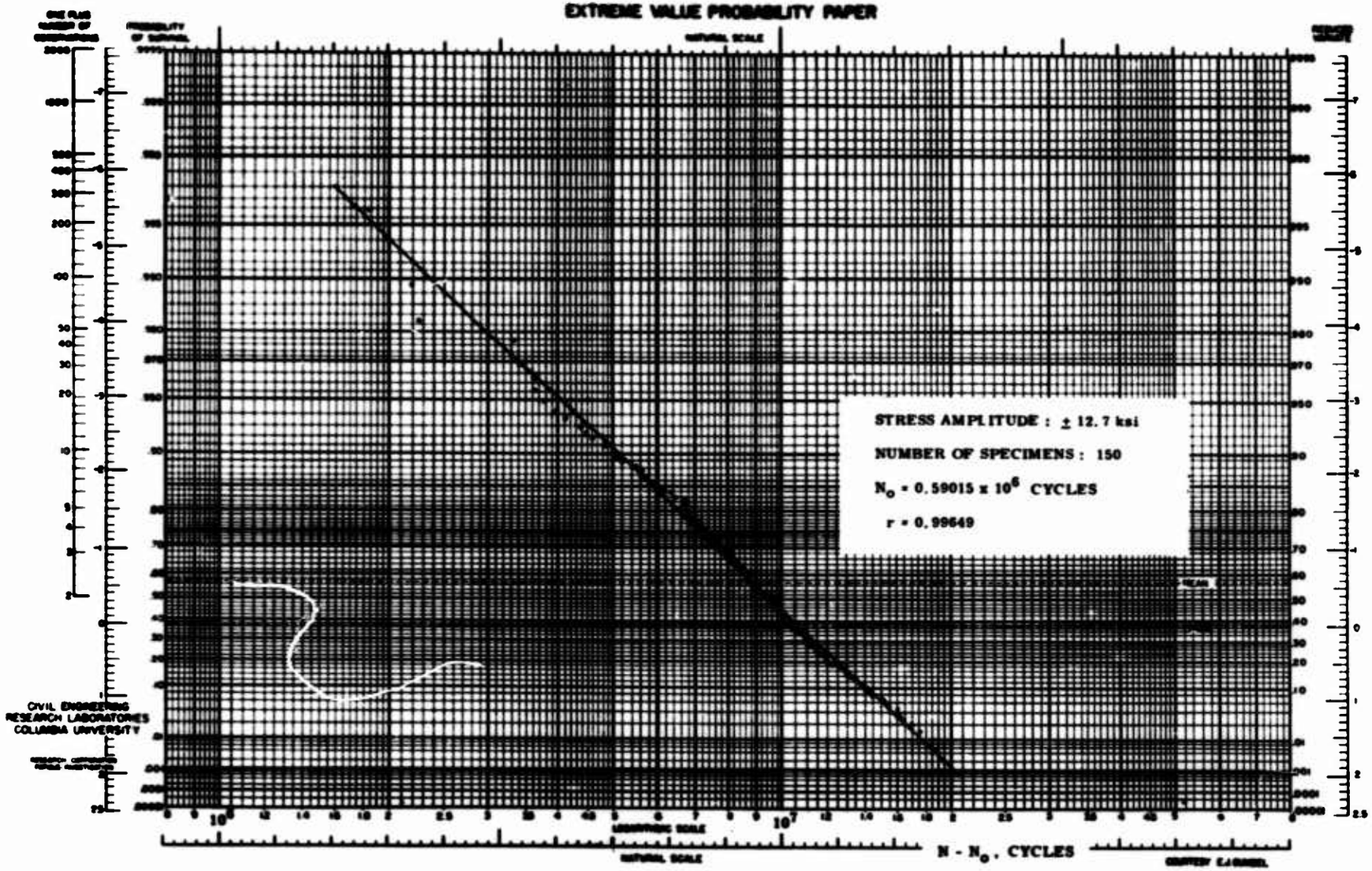

FIG. 13 WEIBULL PROBABILITY PLOT, SINGLE DISTRIBUTION. PARAMETERS CALCULATED BY THE UPPER VERTICAL MOMENT METHOD.

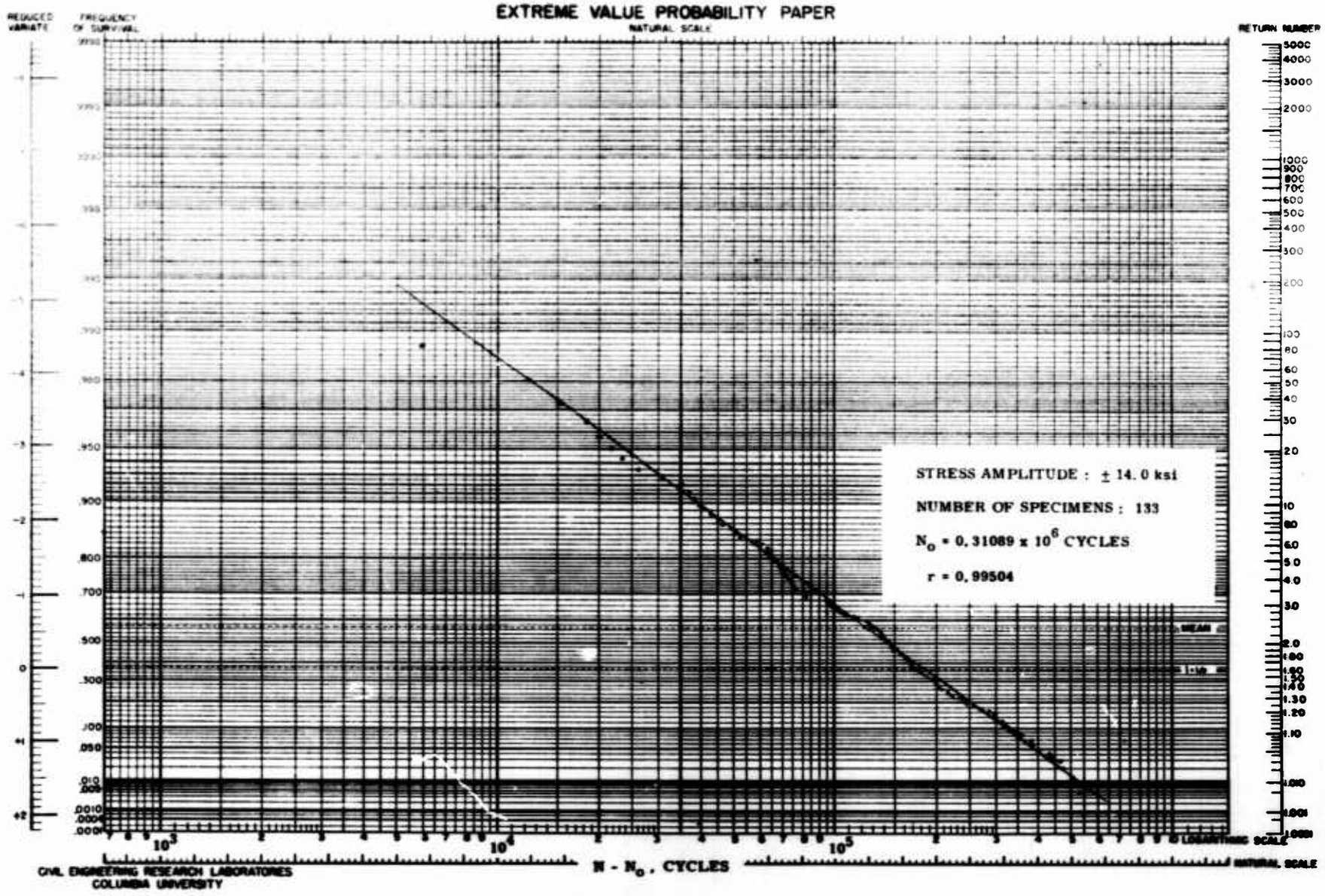

FIG. 14 WEIBULL PROBABILITY PLOT, SINGLE DISTRIBUTION. PARAMETERS CALCULATED BY THE UPPER VERTICAL MOMENT METHOD.

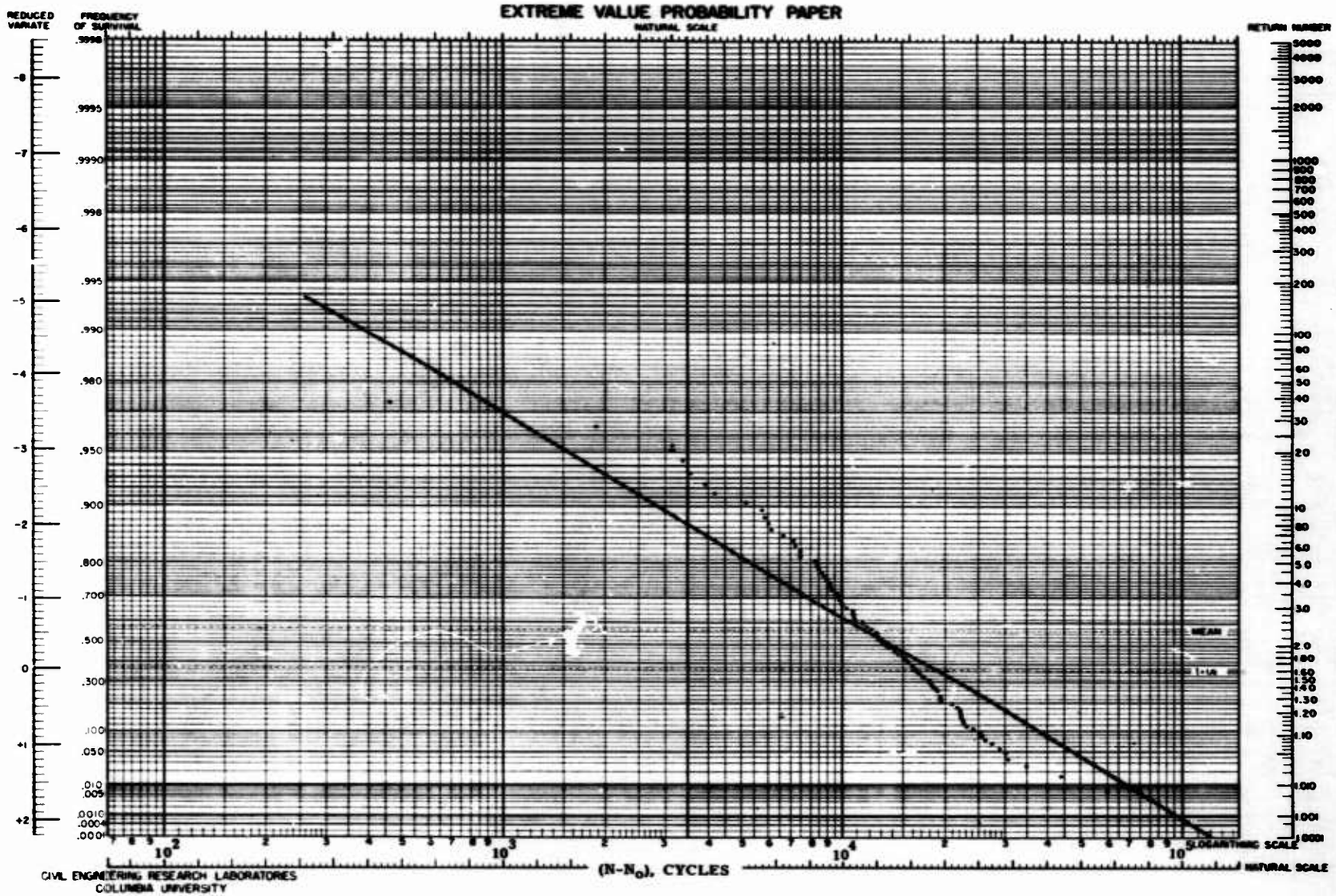

FIG. 15 WEIBULL PROBABILITY PLOT, SINGLE DISTRIBUTION. PARAMETERS CALCULATED BY UPPER VERTICAL MOMENT METHOD. 19.0 KSI, 100 SPECIMENS, r=0.88723.

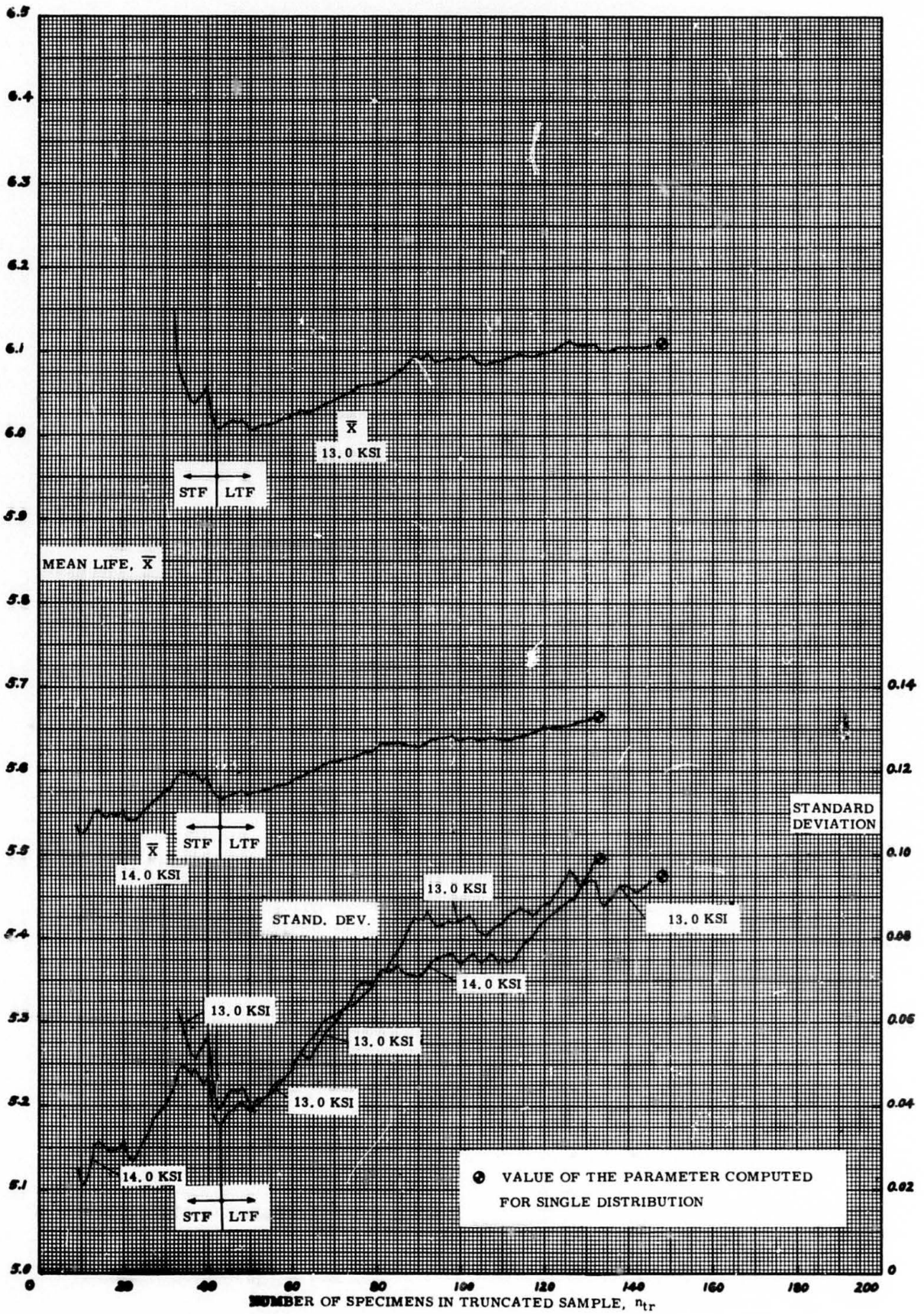

FIG. 16 PARAMETERS OF THE TRUNCATED LOG-NORMAL DISTRIBUTION. HIGH-ENDURANCE PART EXCLUDED. 13.0 KSI AND 14.0 KSI STRESS LEVELS

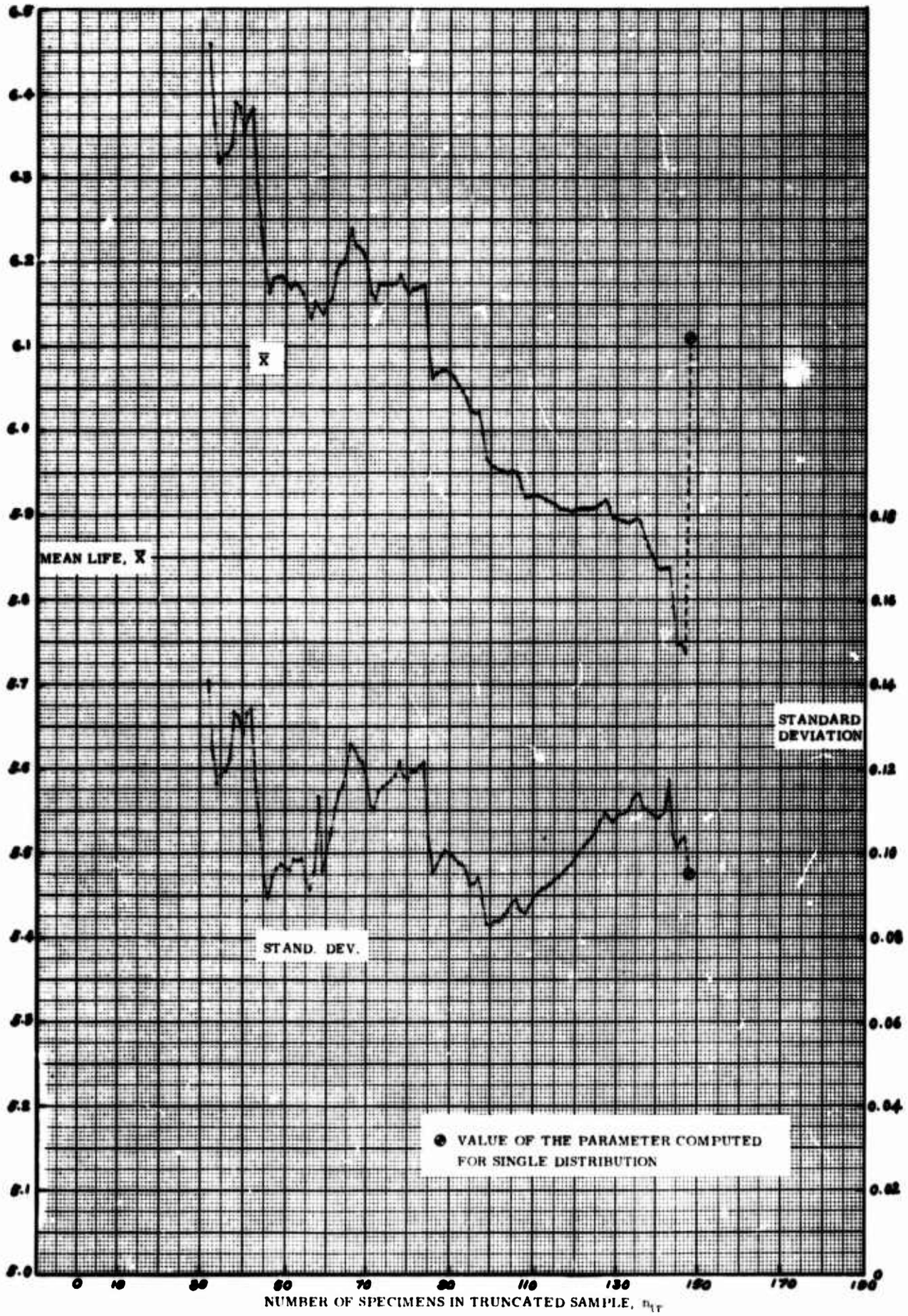

FIG. 17 PARAMETERS OF THE TRUNCATED LOG-NORMAL DISTRIBUTION. LOW-ENDURANCE PART EXCLUDED. 13.0 KSI STRESS LEVEL

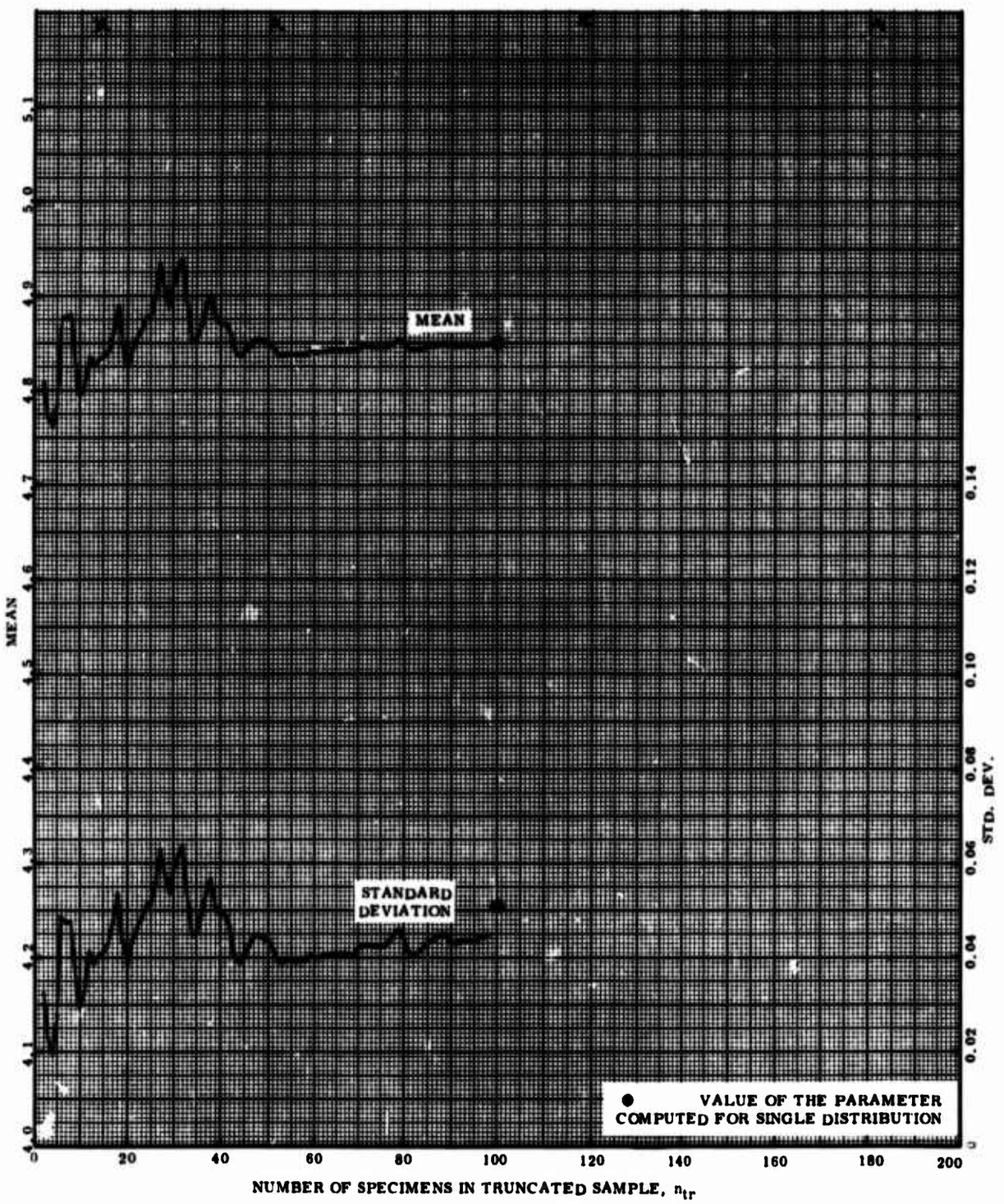

FIG. 18 PARAMETERS OF THE TRUNCATED LOG-NORMAL DISTRIBUTION. HIGH ENDURANCE PART EXCLUDED. 19.0 KSI STRESS LEVEL.

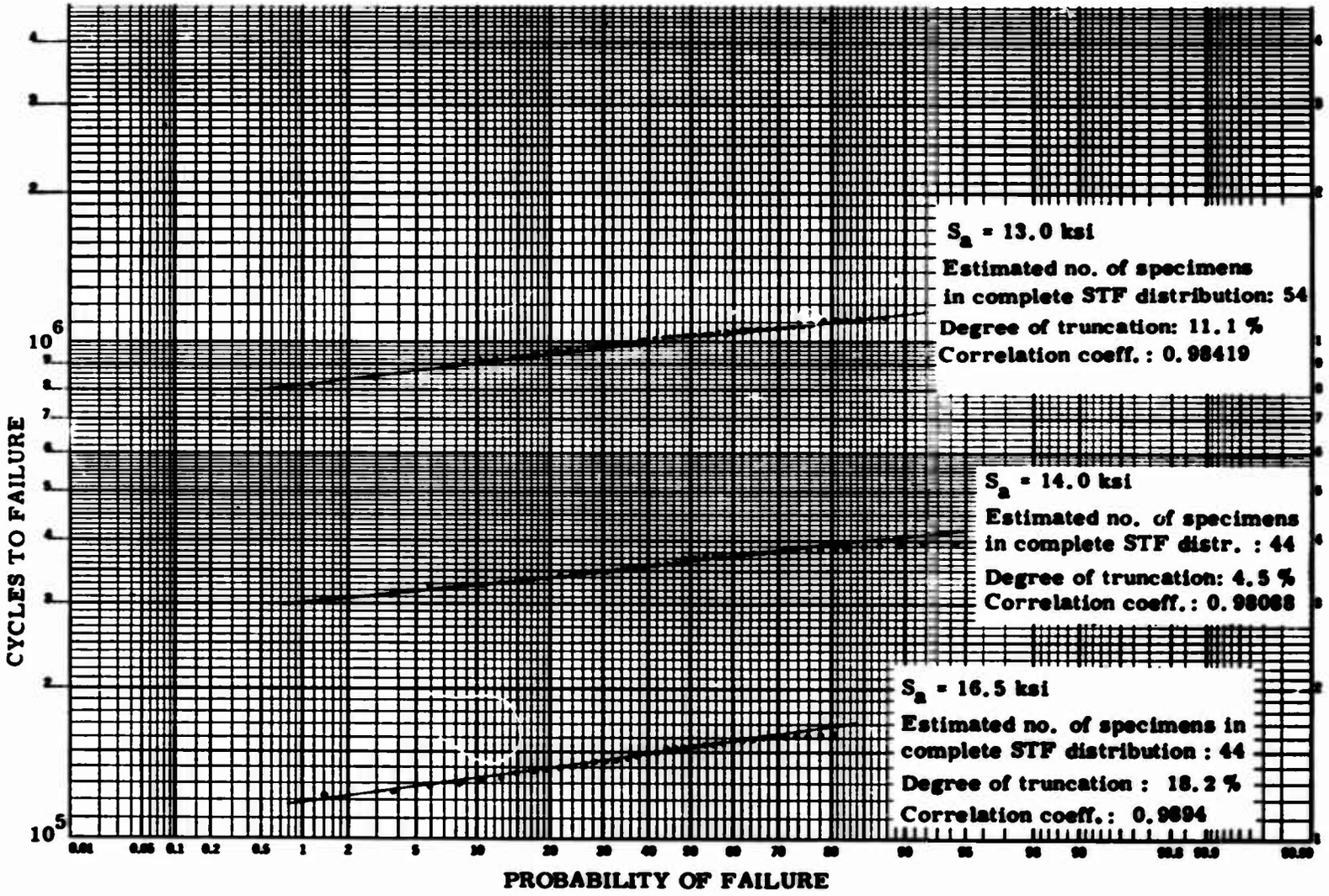

FIG 19 TWO-DISTRIBUTION PRESENTATION OF RESULTS. LOG-NORMAL PROBABILITY PLOTS OF STF COMPONENT DISTRIBUTION.

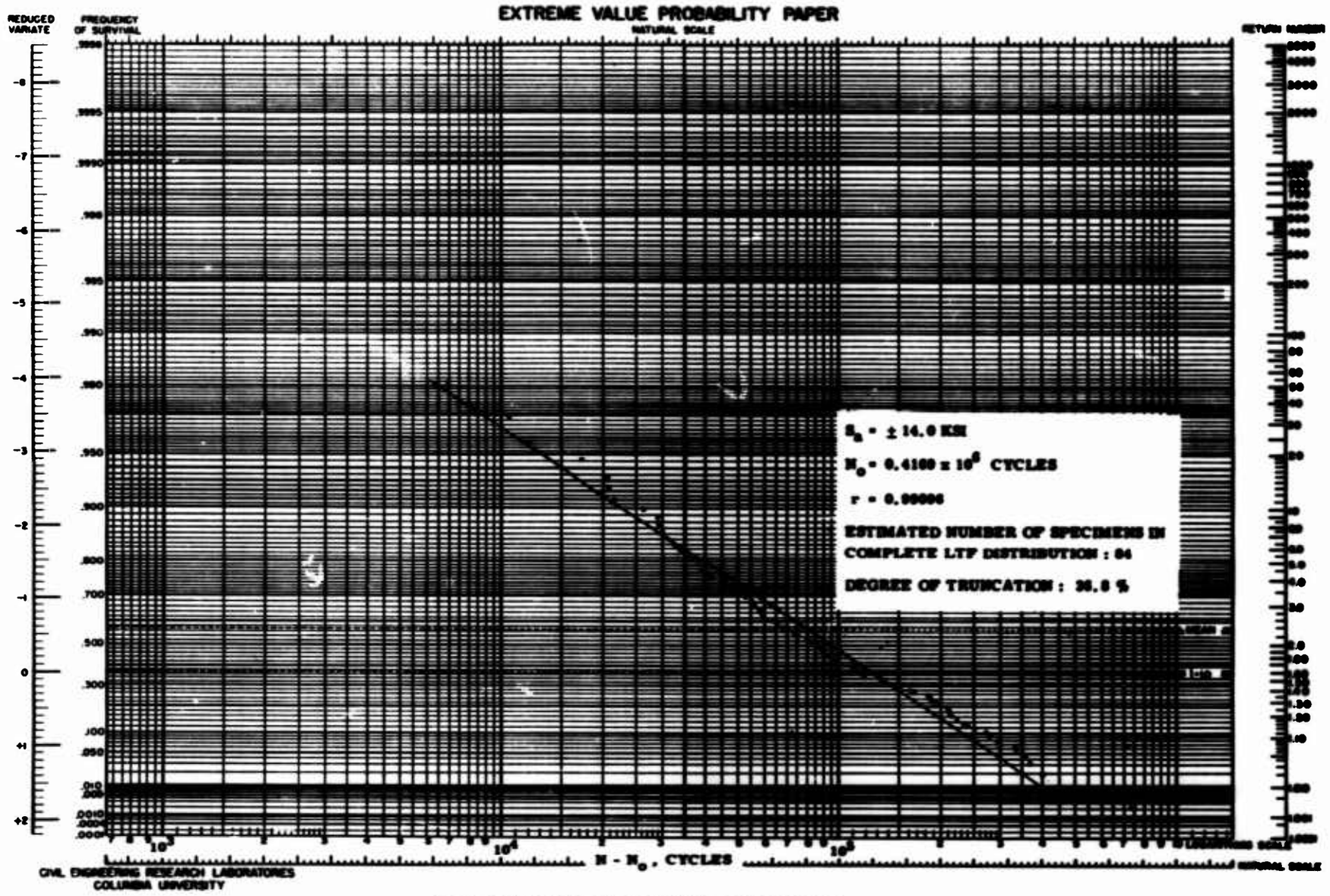

FIG. 20 TWO-DISTRIBUTION PRESENTATION OF RESULTS.
WEIBULL PROBABILITY PLOT OF HIGH-ENDURANCE (LTF) COMPONENT.
PARAMETERS CALCULATED BY THE UPPER VERTICAL MOMENT METHOD.

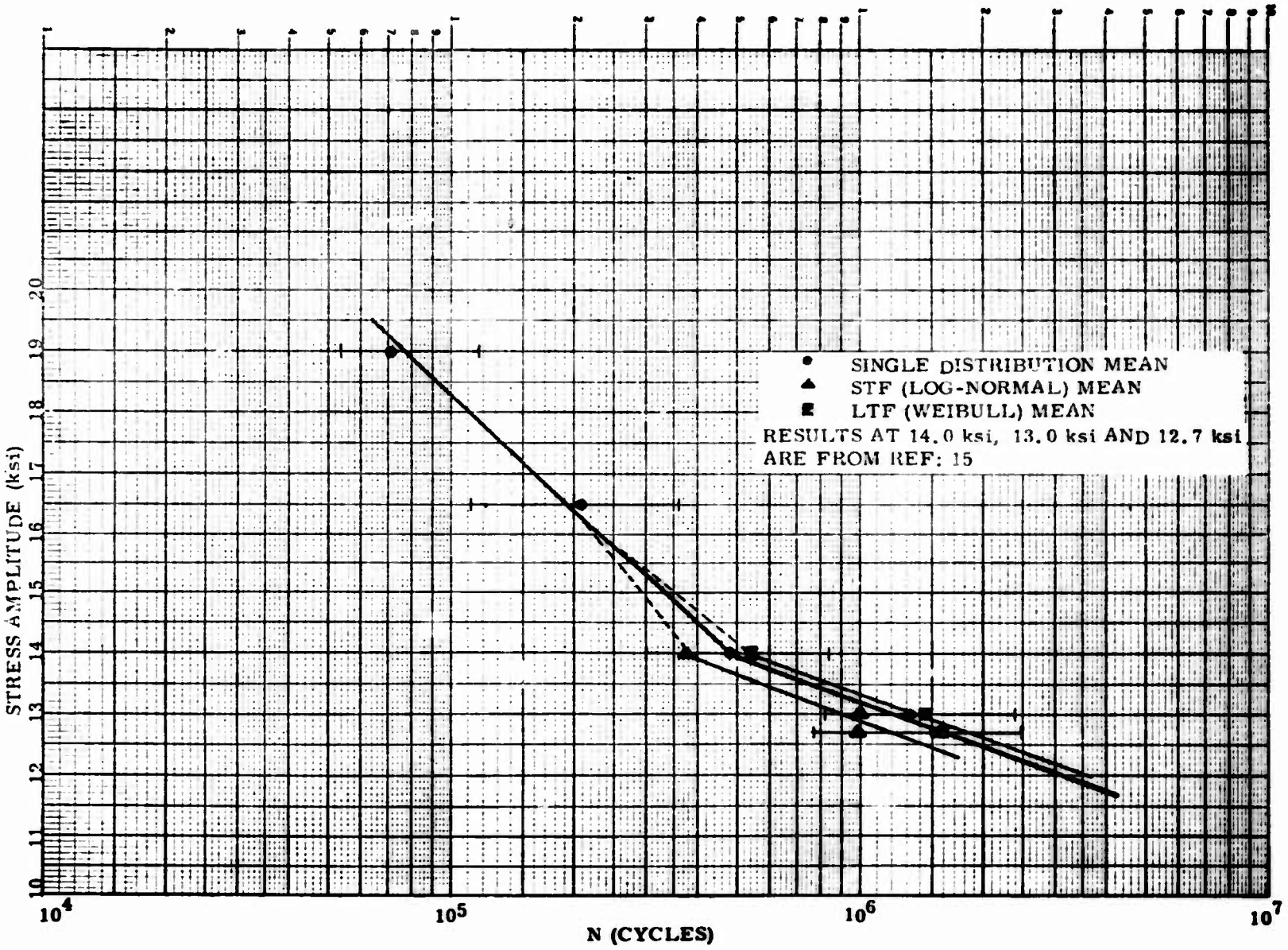

FIG. 21 SCHEMATIC REPRESENTATION OF S-N CURVE WITH SCATTER RANGES AND DISTRIBUTION MEANS.

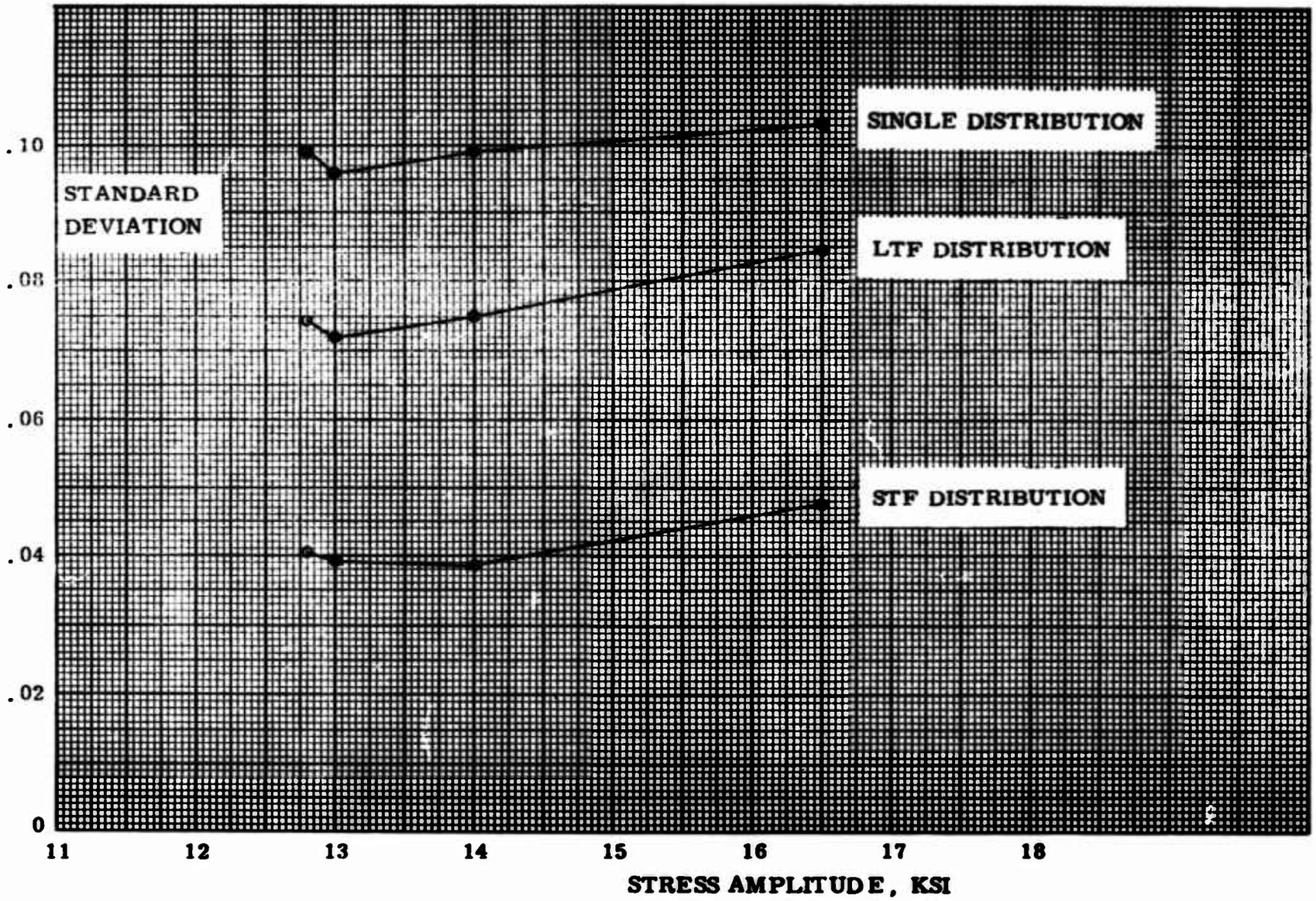

FIG. 22 VARIATION IN STANDARD DEVIATION WITH STRESS AMPLITUDE

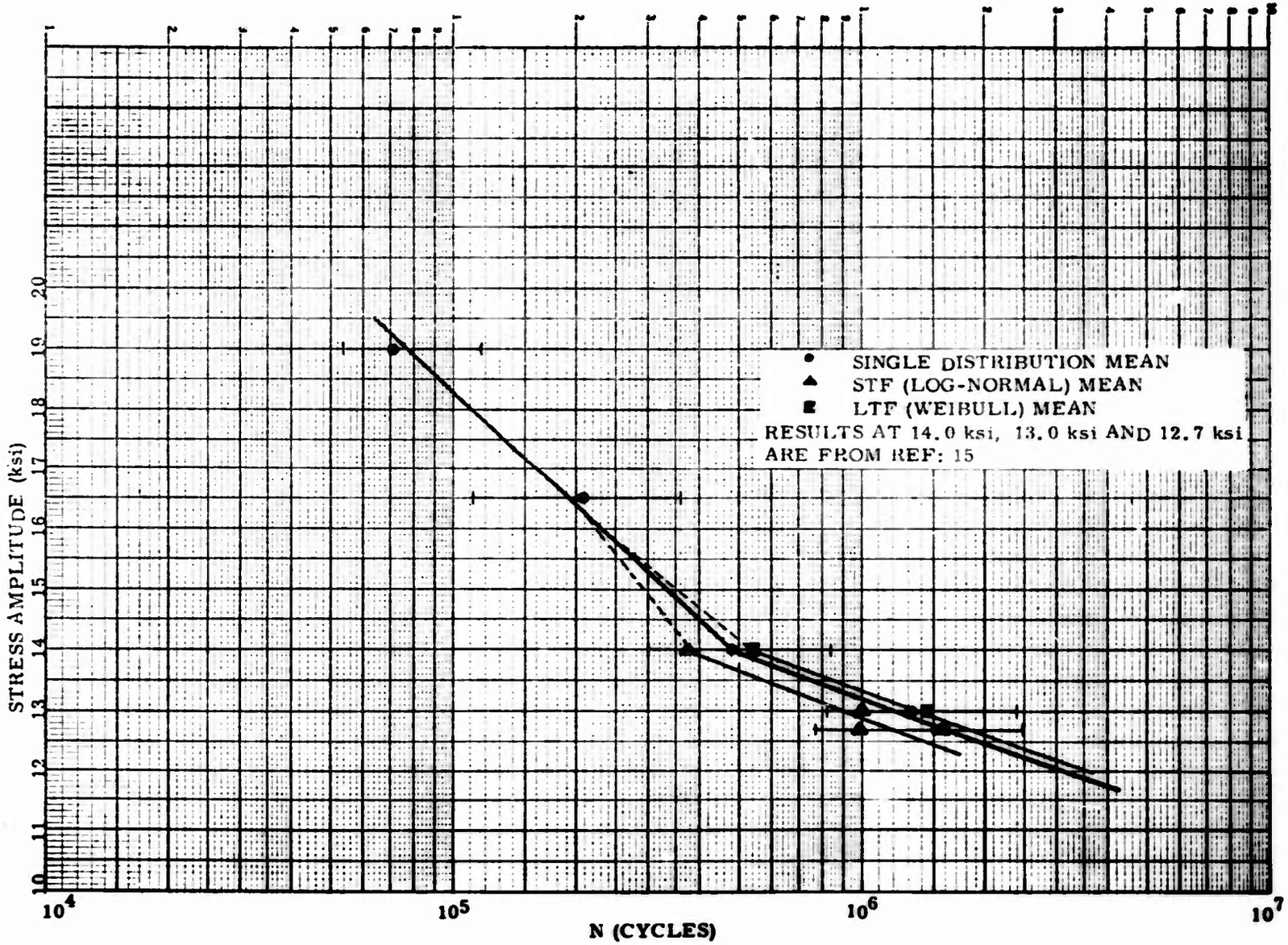

FIG. 21 SCHEMATIC REPRESENTATION OF S-N CURVE WITH SCATTER RANGES AND DISTRIBUTION MEANS.

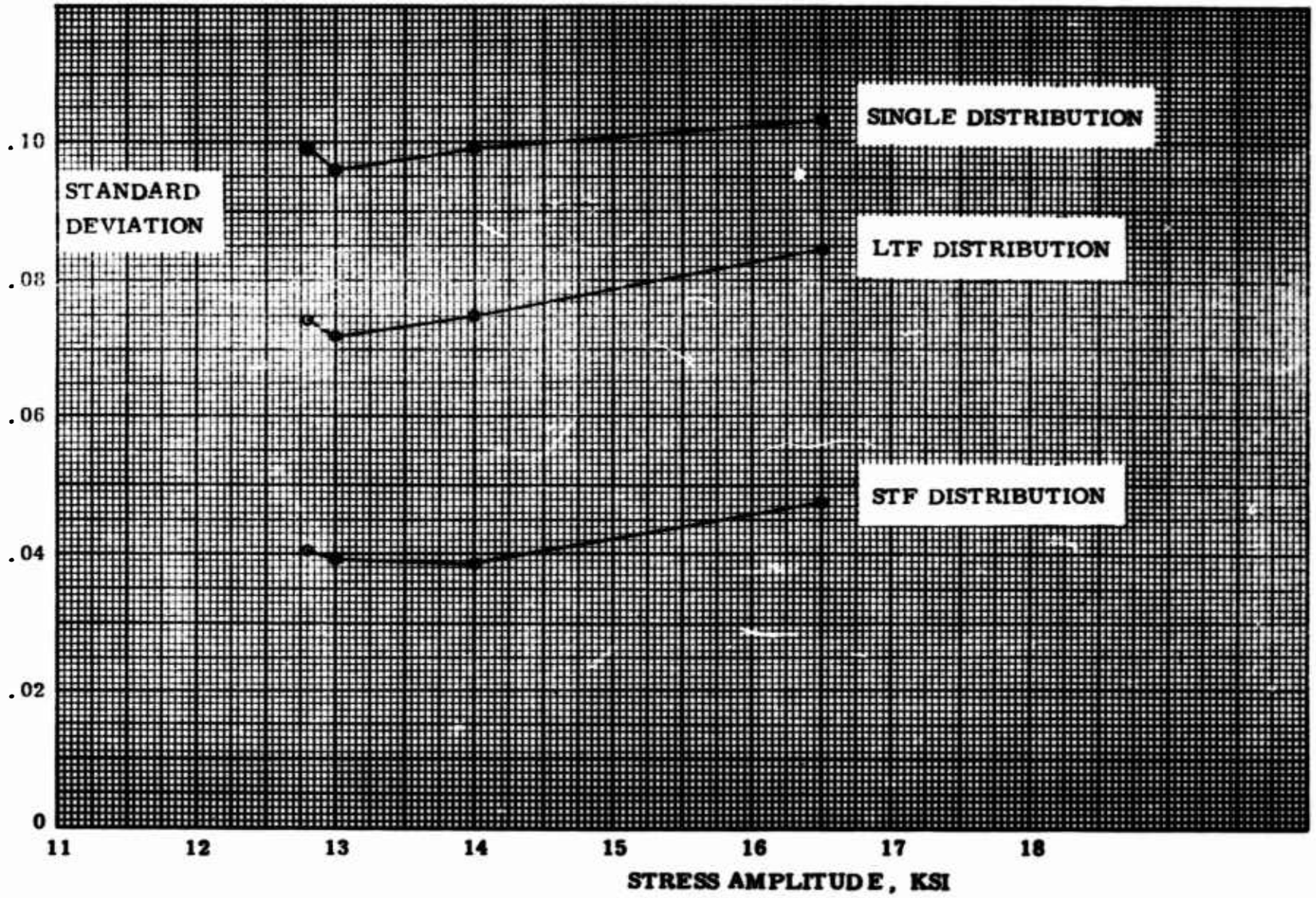

FIG. 22 VARIATION IN STANDARD DEVIATION WITH STRESS AMPLITUDE

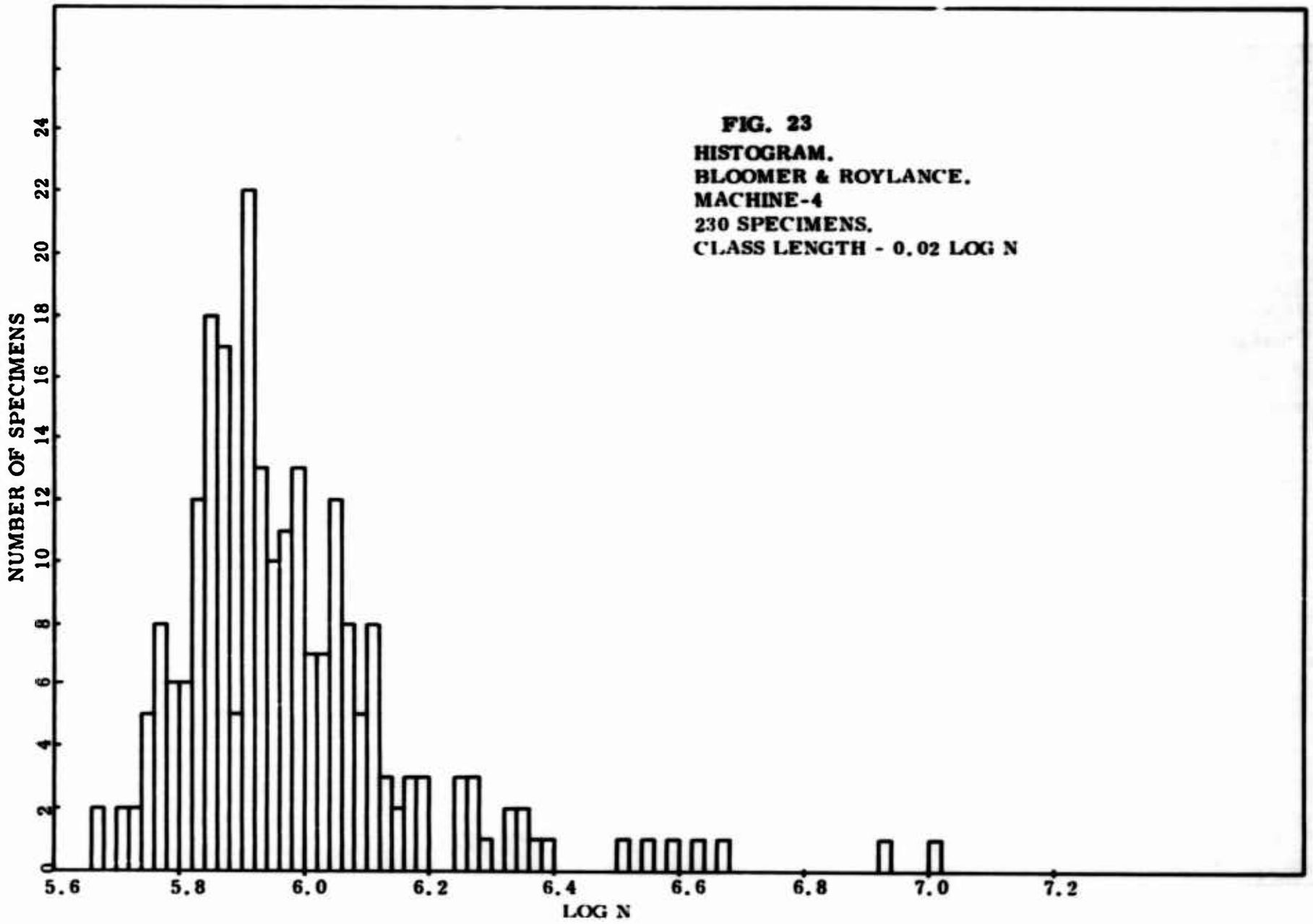

FIG. 23
HISTOGRAM.
BLOOMER & ROYLANCE.
MACHINE-4
230 SPECIMENS.
CLASS LENGTH - 0.02 LOG N

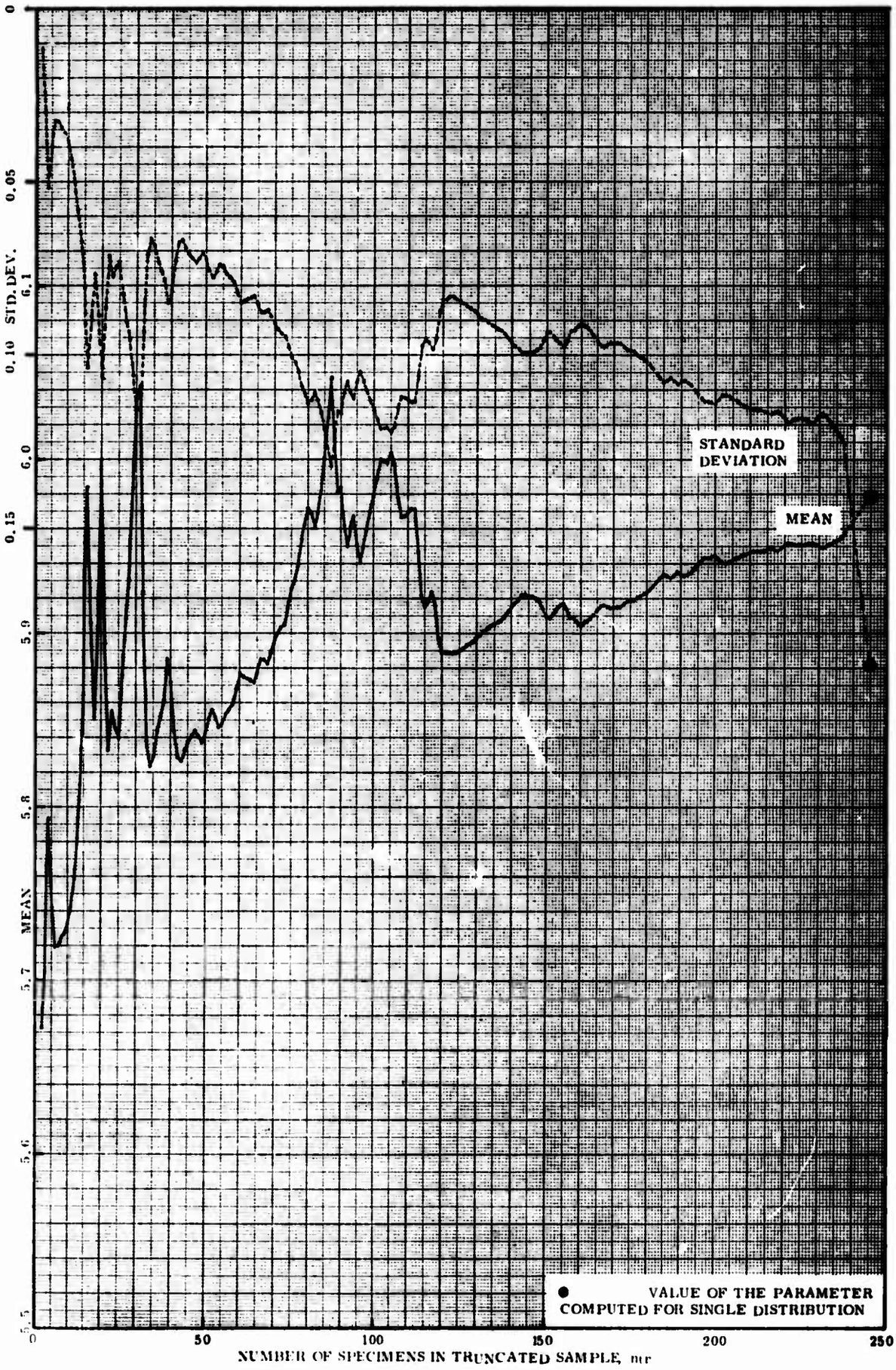

FIG. 24 PARAMETERS OF THE TRUNCATED LOG-NORMAL DISTRIBUTION, HIGH ENDURANCE PART EXCLUDED. BLOOMER & ROYLANCE, MACHINE - 3.

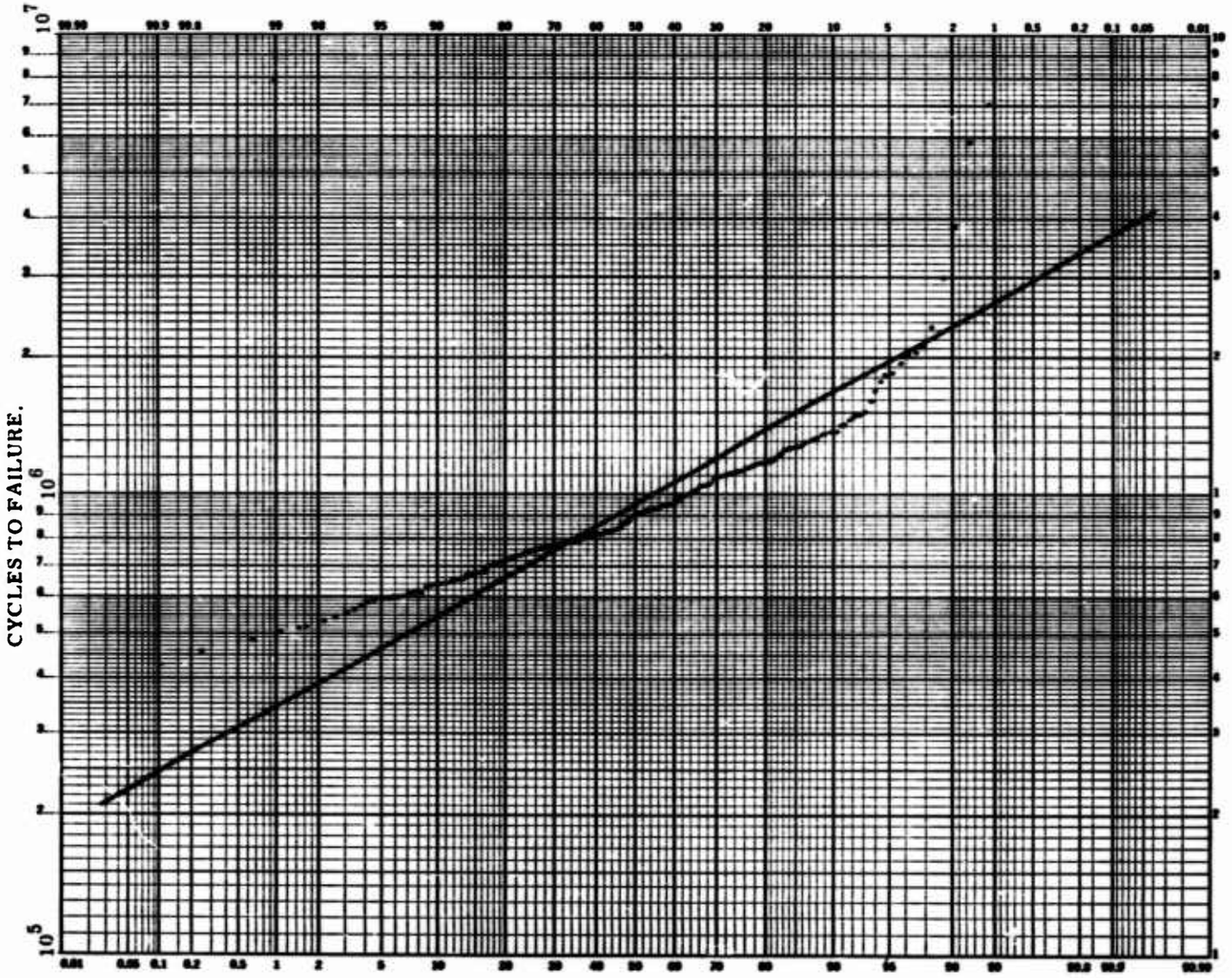

FIG. 25 LOG-NORMAL PROBABILITY PLOT. SINGLE DISTRIBUTION. BLOOMER & ROYLANCE, MACHINE-3; 245 SPECIMENS, r=0.88778.

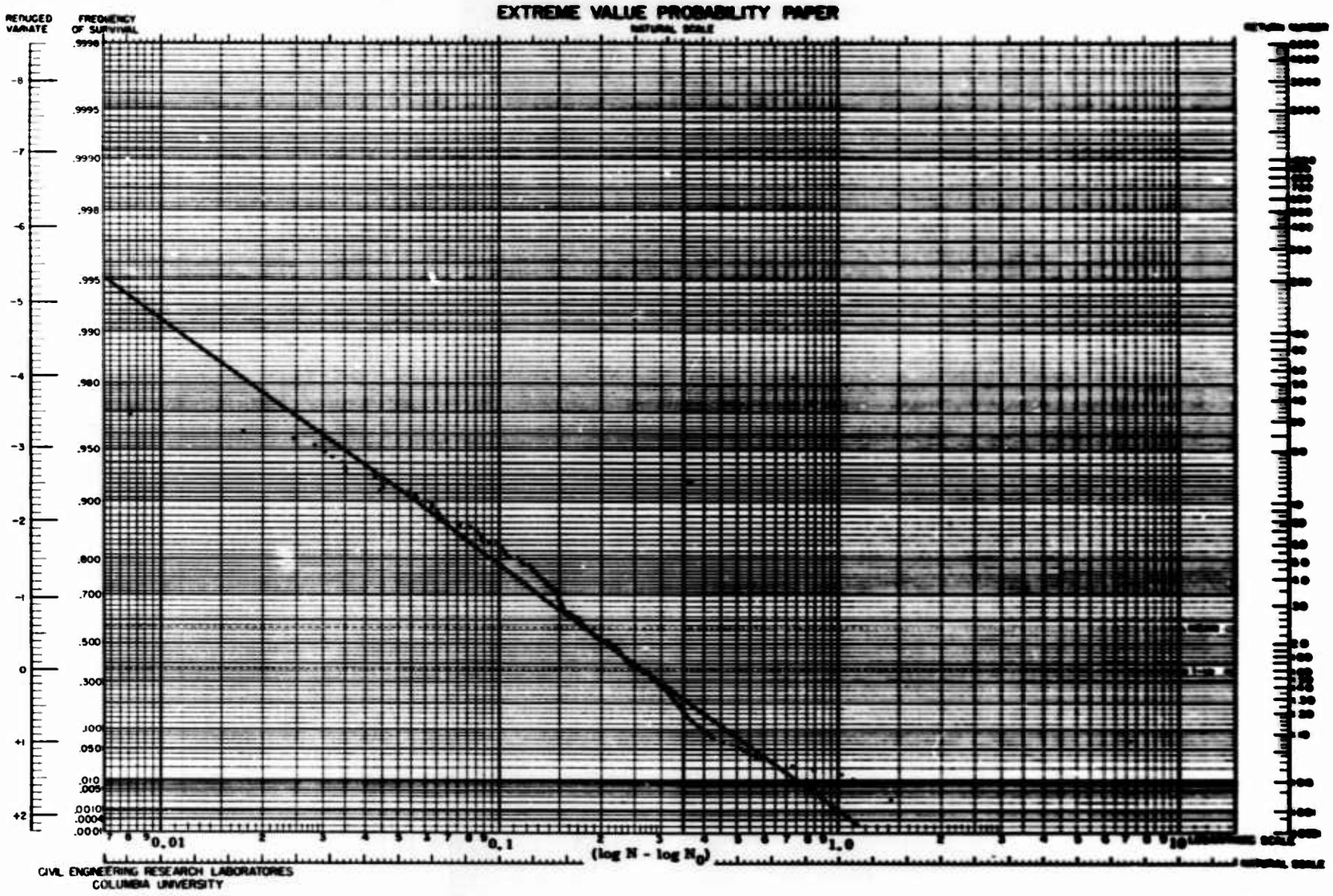

FIG. 26 LOG-WEIBULL PROBABILITY PLOT. SINGLE DISTRIBUTION. PARAMETERS CALCULATED BY UPPER VERTICAL MOMENT METHOD. BLOOMER AND ROY LANCE, MACHINE-3, 245 SPECIMENS, $\log N_0 = 6.00701$.

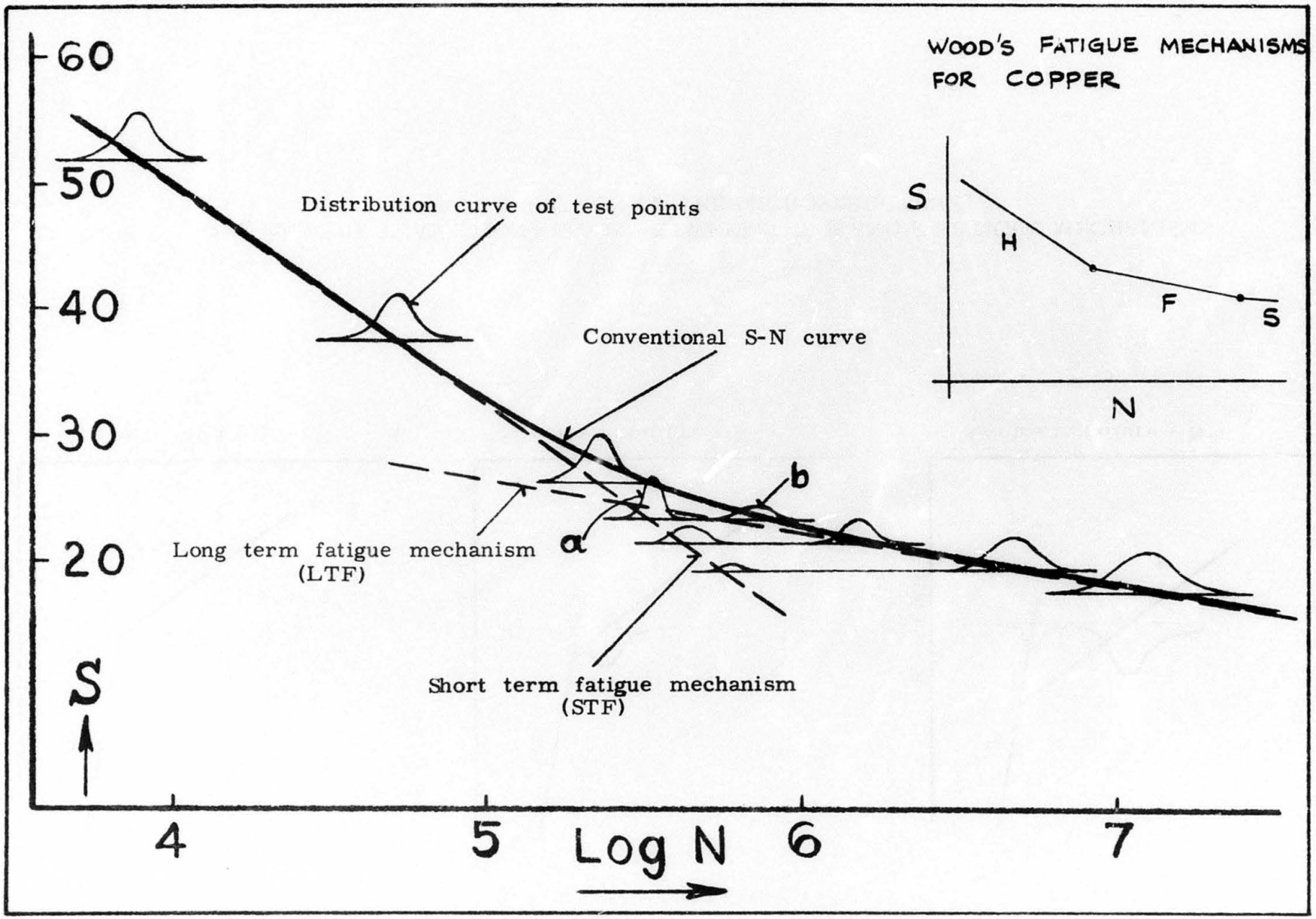

FIG, 27 SWANSON'S TWO DISTRIBUTION INTERPRETATION OF HIS FATIGUE TEST RESULTS

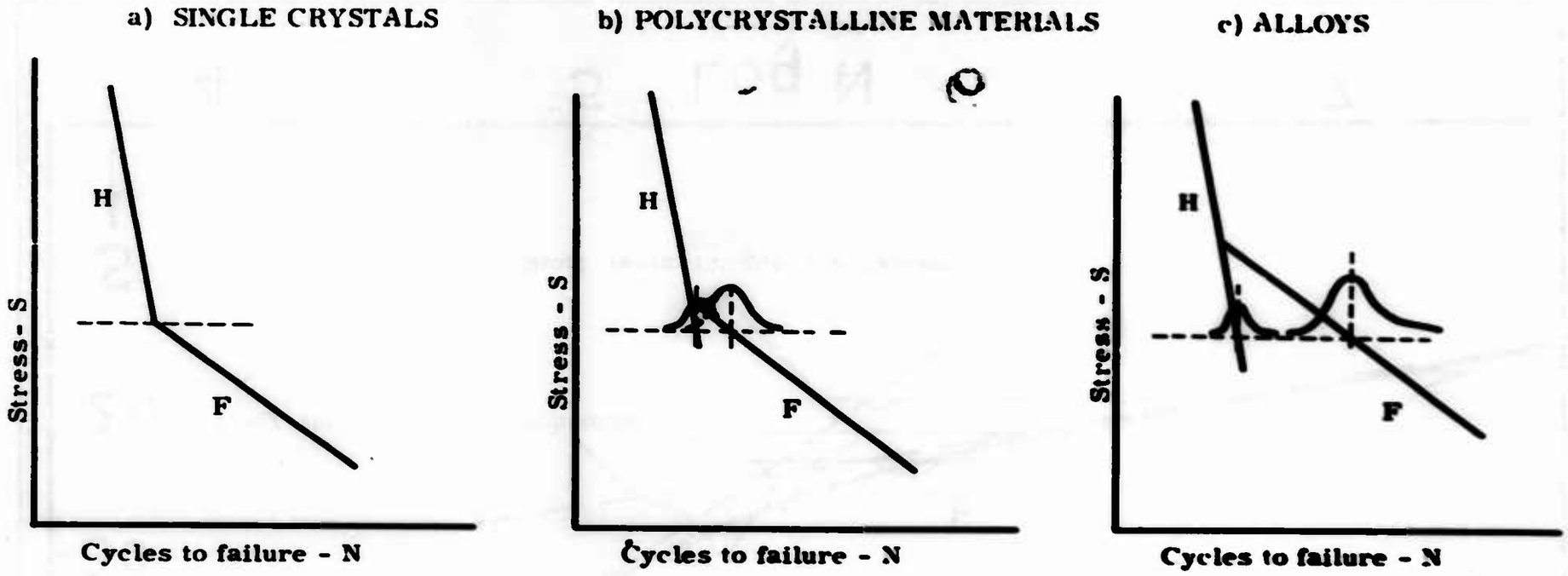

FIG. 28 THE TRANSITION REGION BETWEEN THE H AND F FATIGUE MECHANISMS AS A FUNCTION OF THE MICROSTRUCTURE.